A Model for the Hedging Impact of Option Market Makers

Sebastian Egebjerg*[a] and Thomas Kokholm†[a,b]

[a]Aarhus BSS, Aarhus University, Department of Economics and Business Economics, Denmark

[b]Danish Finance Institute

[b]Center for Research in Energy: Economics and Markets

Abstract

We propose a model that embeds a directional price impact when Option Market Makers (OMMs) delta hedge their option inventory. In extension of existing theoretical contributions that focus on the gamma effect, we include an additional impact when changes to the option inventory are hedged by the OMM (the inventory effect). When the fundamental value of the stock has constant volatility and drift terms, inclusion of a hedging impact implies that the observable stock price features both stochastic volatility and stochastic drift. Analyzing the gamma-induced price impact in isolation can underestimate the total effect when the OMM's inventory adjustments reinforce the gamma impact and overestimate it when the adjustments move in the opposite direction. Using a high-frequency data set on SPX option trades, we estimate changes to the net option position of OMMs over an extended period and find that the change is closely linked to subsequent SPX futures returns. A decomposition of the net delta change into changes due to the gamma effect as well as the inventory effect reveals that both quantities are significant and with impact in line with the model predictions.

Keywords: Price impact, option hedging, frictions, feedback effects

JEL codes: G12, G13, G14, G23

*seeg@econ.au.dk

†thko@econ.au.dk

Contents

1 Introduction

The role of option market makers (OMMs) in shaping market dynamics has received increased attention in recent years. Especially, following the volatile market conditions of the Corona pandemic, debates have unfolded in academic and mainstream journals regarding the extent of the impact of market makers' hedging activities on heightened stock price volatility. OMMs provide liquidity to the market by taking the opposite side of any unmatched option orders and profit from the flow of transactions. To effectively manage risk, OMMs need to delta hedge their unbalanced option positions by trading the underlying asset. Hence, this creates a channel by which the price of the securities underlying the options is impacted by option trading, depending on the size of the delta hedge and the depth of the market. Moreover, it is empirically documented that the OMM's aggregated net option position is commonly short, resulting in a negative gamma exposure. This position implies trading in the same direction as market movements, which effectively intensifies both upward and downward price swings (Baltussen et al. 2021, Barbon and Buraschi 2020, Barbon et al. 2021, Ni et al. 2021). Consequently, their hedging activities influence market fragility, highlighting the importance for all market participants to understand the implications.

The present paper contributes to two interlinked strands of literature. First, we model the relationship between OMMs' hedging activities and the dynamics of the underlying asset to examine the resulting price impact on the underlying asset. This work relates to the model developed by Sornette et al. (2022). However, their model accounts only for the gamma effect, namely, the rebalancing of delta hedges stemming from price changes to the underlying asset. We allow the option inventory of the OMM to be stochastic and extend the approach by embedding a stock price impact when changes to the option inventory are delta hedged. Thus, our model accounts for price impacts through OMMs delta hedging adjustments to their existing aggregate delta position (gamma effect) and the explicit changes to their option inventory (inventory effect).

Figure 1 illustrates these two channels when the OMM holds a net short aggregate option

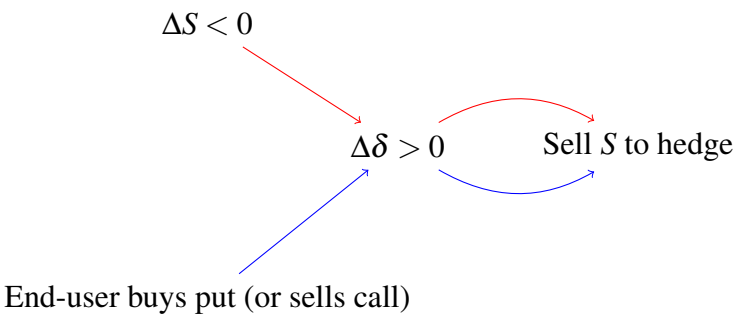

Figure 1: Hedging channels leading to selling pressure when the OMM holds a negative aggregate gamma position.

position, implying a negative gamma exposure. A short rebalancing hedge can be triggered in two ways: First, by a decline in the underlying asset (gamma effect), or second, by end-users buying puts or selling calls (inventory effect). When both forces act in the same direction, they reinforce one another and amplify the overall price impact on the underlying. Naturally, it can also be the case that the two channels work in opposite directions.

In our model, when the fundamental value of the asset has constant drift and volatility terms, the inclusion of a linear price impact of trades leads to an observable stock price featuring both stochastic volatility and drift terms. We estimate the model on high-frequency SPX option data and deduce a number of observations from a subsequent simulation analysis. The analysis highlights that focusing on the price impact implied by the gamma effect in isolation will underestimate the impact in scenarios where the OMM's option inventory changes in a direction that implies trading in the same direction, while it will overestimate it when the adjustments move in the opposite direction. Second, in comparison to other studies, we advance the empirical literature on the hedging impact of market makers on the stock market utilizing the SPX options data to more accurately infer the option inventory of OMMs. For instance, Baltussen et al. (2021), Barbon and Buraschi (2020), Bangsgaard and Kokholm (2024) impose the simplifying assumption that end-user demand in puts is long while the demand in calls is short and use variations in the option open interest to quantify the imbalance of the market maker. Notably, our methodology addresses the limitations of existing research, by using a novel trade classification algorithm tailor-made for high-frequency SPX option trade data (Grauer et al.

2023). The algorithm is designed to remedy shortcomings of existing trade classification algorithms. We also apply a more conventional classification approach to confirm the robustness of our results.

In line with Baltussen et al. (2021), our empirical study focuses on the delta hedging activities of the market maker in the last 30 minutes of the trading day. A number of reasons for focusing on the end-of-day price impact can be put forward. First, instead of delta hedging during the day, the OMM might try to manage the risk by setting prices in a way that works towards a more balanced option inventory (Ho and Stoll 1981, Grossman and Miller 1988). However, to protect against overnight risk, the OMM should delta hedge any unbalanced option exposure by the market close. As the SPX options trade extensively until the market close at 16.15, it makes sense to postpone hedging until the suggested time slot. Second, holding unhedged option positions overnight triggers additional capital requirements (Hong and Wang 2000). Third, by postponing the hedge, the OMM can benefit from the relatively higher market depth at the end of the day (Baltussen et al. 2021). We confirm previous studies by showing that the required delta hedge, determined by the market maker's option inventory, is a significant predictor of the end-of-day return in SPX futures. Moreover, we decompose the net delta hedge into its part related to changes in the underlying (the gamma effect) and a part related to changes in the option net position (the inventory effect), and provide novel evidence that in scenarios where the two effects work in the same direction, the trading impact will be underestimated if one focuses entirely on the gamma effect and vice versa. All of the results are robust to the inclusion of various control factors.

It is likely that in some cases the shocks to the option inventory will be too large to defer risk management until the end of the day, triggering the market maker to engage in intraday hedging, which will cause immediate price pressure. On the 5-minute frequency, we show that the largest absolute changes to the net delta position are followed by a reaction in the SPX futures return signed in accordance with the hedging direction. Additionally, considering a decomposition of the delta hedging effect, we find evidence that high-frequency intraday hedging is primarily driven by significant changes to the option inventory rather than fluctuations of the underlying.

Thus, our paper also relates to the growing literature on intraday price patterns (Baltussen et al. 2021, Goyenko and Zhang 2019, Muravyev and Ni 2020, Gao et al. 2018, Heston et al. 2010) and in particular Barbon and Buraschi (2020) who show that gamma hedging drives intraday hedging in individual stocks during the trading day.

Moreover, the paper is related to the literature on stock-pinning, namely that delta hedging of OMMs can push the price of the underlying security to the strike price at the maturity of a given option issue with large open interest (Avellaneda and Lipkin 2003, Ni et al. 2005, Golez and Jackwerth 2012). Hence, available empirical evidence points to the possibility that hedging activities by option market makers can influence the market for the underlying security. In the present work, we focus on the directional impact of delta hedging of the aggregate option exposure of OMMs.

Another related portion of the literature investigates the inter-linkage between option prices and the option inventory of OMMs. Most prominently, Garleanu et al. (2008) develop a model to capture how demand pressure affects option pricing, and Bollen and Whaley (2004) show that net buying pressure is directly related to changes in the option implied volatility. Building on this work, Jacobs and Mai (2024) confirm the findings in Bollen and Whaley (2004) regarding the positive relationship between net option demand and option prices in the SPX market. While we deal with the impact of market maker inventory management, we focus on the impact on the price of the underlying asset rather than option prices.

A number of empirical studies examine the role of hedging activities in facilitating price discovery in financial markets. For instance, Hu (2014) finds that the order flow in options has predictive impact on the underlying stock price via the OMM's hedging activities. In contrast, Chen et al. (2016) find that trades in index options do not contribute to price discovery. Baltussen et al. (2021) study the gamma effect and find evidence of return reversals following the closure of the hedging window, defined as the last half hour of the trading day, indicating that price changes related to the gamma effect are not informative. We combine both these effects in a theoretical setting and study empirically both the option inventory effect and the gamma effect.

The remainder of the paper is structured as follows: Section 1 introduces the model and derives closed form expressions for the drift and volatility terms of the observed stock price. Next, Section 3 presents the trade classification algorithm and provides an estimation of the model. Moreover, a simulation analysis of the model is included. In Section 4, different regression models are considered, and evidence is presented in support of the presence of the market maker's hedging impact. Finally, we conclude in Section 5.

2 Theoretical framework

We consider a stock with price S_t and with an active market for European options traded on it. We assume the existence of an Option Market Maker (OMM) that provides liquidity to the market and takes the opposite position of all option trades initiated by the end-users in the economy. The OMM has limited risk absorbing capacity and chooses to hedge a fixed fraction $h \in [0,1]$ of the option inventory.[1] In addition, we assume that the end-users refrain from hedging. We allow the hedging activities of the OMM to impact the price of the stock leading to a departure of the observable stock price from the fundamental value of the stock. The OMM hedges the option positions by trading the underlying security in a quantity that matches the Black-Scholes delta of the options δ_t. In Section 2.1, we develop the model based on the assumption that calls are the only type of options traded. Next, in Section 2.2, we relax this assumption and add put options to the market.

2.1 Stock price dynamics when delta-hedged call options are traded

Consider a filtered probability space $\left(\Omega, \mathcal{F}, (\mathcal{F}_t)_{t\geq 0}, \mathbb{P}\right)$, where $(\mathcal{F}_t)_{t\geq 0}$ is the completed right-continuous natural filtration generated by a two-dimensional Brownian motion $\left(W_t^F, W_t^C\right)$ with instantaneous correlation $dW_t^F dW_t^C = \rho dt$. Similar to Sornette et al. (2022), we model the unobservable fundamental value of the stock price F_t as a geometric Brownian motion. Hence,

[1] An OMM may choose to hedge only partially for several reasons, including speculative considerations, the ability to offset incoming option flows, and the presence of transaction costs.

the log value $f_t = \log F_t$ has dynamics

$$df_t = \alpha dt + \nu dW_t^F, \tag{1}$$

where $\nu \geq 0, \alpha \in \mathbb{R}$, and W_t^F represents the fundamental shocks to the economy.

Here we consider the case when a single type of call options are traded in the market all sharing the same strike K and maturity τ. Let N_t denote the net option inventory of the OMM (positive if long and negative if short). The inventory risk is governed by the call option order flow assumed to follow a Brownian motion

$$dN_t = \nu^C dW_t^C, \tag{2}$$

where $\nu^C \geq 0$. The OMM's time-t position in the underlying asset implied by the hedging strategy equals

$$V_t = -h\delta_t N_t. \tag{3}$$

The impact from delta hedging is the only friction in the model, and we assume that the observed log price change ds_t is the sum of the change in the log of the fundamental price and the hedging volume ΔV_t scaled by a constant $\beta \geq 0$ (linear price impact)

$$ds_t = d\log S_t = df_t + \beta dV_t \quad \text{for} \quad t \in \mathcal{T}_\varepsilon, \tag{4}$$

where for some small $\varepsilon > 0$ the set $\mathcal{T}_\varepsilon$ is defined as

$$\mathcal{T}_\varepsilon = \{t \geq 0 \mid 1 + \beta h N_t S_t \gamma_t \geq \varepsilon\}.$$

The imposition that $t \in \mathcal{T}_\varepsilon$ in (4) is a technical condition done in order to ensure that the model construction (4) is well-defined. Later, we will extend the model to also include the case when $t \notin \mathcal{T}_\varepsilon$. This specification captures that departures of S_t from the fundamental value F_t are induced by inventory driven hedging demand of the OMM. From Itô's product rule we have

that the hedging volume has dynamics (Protter (1990), Corollary 2)

$$dV_t = -h\left(N_t d\delta_t + \delta_t dN_t + dN_t d\delta_t\right). \tag{5}$$

Denote by σ_t^{IV} the time-t implied volatility of the option. An application of Itô's Lemma on the option delta $\delta_t = \delta(t, S_t, \sigma_t^{IV})$ reveals that

$$\begin{aligned} d\delta_t =& \frac{\partial \delta_t}{\partial t} dt + \frac{\partial \delta_t}{\partial S_t} dS_t + \frac{1}{2} \frac{\partial^2 \delta_t}{\partial (S_t)^2} (dS_t)^2 \\ &+ \frac{\partial \delta_t}{\partial \sigma_t^{IV}} d\sigma_t^{IV} + \frac{1}{2} \frac{\partial^2 \delta_t}{\partial \left(\sigma_t^{IV}\right)^2} \left(d\sigma_t^{IV}\right)^2 + \frac{\partial^2 \delta_t}{\partial S_t \partial \sigma_t^{IV}} dS_t d\sigma_t^{IV} \\ \approx& \chi_t dt + \gamma_t dS_t + \frac{1}{2} \psi_t (dS_t)^2, \end{aligned} \tag{6}$$

where we in the approximation ignore the terms arising due to the Black-Scholes implied volatility not being constant over time. Here, $\chi_t = \frac{\partial \delta_t}{\partial t}$ is known as the delta decay, i.e., the rate at which the delta of the option changes with respect to time, and $\psi_t = \frac{\partial^2 \delta_t}{\partial S_t^2}$ measures the sensitivity of the option gamma, $\gamma_t = \frac{\partial \delta_t}{\partial S_t}$, to changes in the underlying asset.

For $t \in \mathcal{T}_\varepsilon$, the modeling equations (1)-(4) imply that the price process dynamics are continuous and driven by $\left(W_t^F, W_t^C\right)$ with

$$dS_t = \mu_t S_t dt + \sigma_t^F S_t dW_t^F + \sigma_t^C S_t dW_t^C, \tag{7}$$

for suitable coefficients μ_t, σ_t^F, and σ_t^C. Hence, the log-price dynamics has the form

$$ds_t = \left(\mu_t - \frac{1}{2}(\sigma_t^S)^2\right) dt + \sigma_t^F dW_t^F + \sigma_t^C dW_t^C \tag{8}$$

where $\sigma_t^S = \sqrt{(\sigma_t^F)^2 + (\sigma_t^C)^2 + 2\sigma_t^F \sigma_t^C \rho}$. Entering the stock price dynamics (7) into the delta dynamics (6) yields

$$d\delta_t \approx \kappa dt + \sigma_t^F S_t \gamma_t dW_t^F + \sigma_t^C S_t \gamma_t dW_t^C, \tag{9}$$

where

$$\begin{aligned}\kappa &= \frac{\partial \delta_t}{\partial t} + \mu_t S_t \frac{\partial \delta_t}{\partial S_t} + \frac{1}{2}(\sigma_t^F)^2 S_t^2 \frac{\partial^2 \delta_t}{\partial S_t^2} + \frac{1}{2}(\sigma_t^C)^2 S_t^2 \frac{\partial^2 \delta_t}{\partial S_t^2} + \sigma_t^F \sigma_t^C S_t^2 \rho \frac{\partial^2 \delta_t}{\partial S_t^2} \\ &= \chi_t + \mu_t S_t \gamma_t + \frac{1}{2}\psi_t S_t^2 (\sigma_t^S)^2. \end{aligned} \tag{10}$$

Combining equation (4) with (9) and (2) yields that

$$\begin{aligned} ds_t = &\left(\alpha - \beta h N_t \kappa - \beta h \nu^C S_t \gamma_t \left(\sigma_t^F \rho + \sigma_t^C\right)\right) dt \\ &+ \left(\nu - \beta h N_t \sigma_t^F S_t \gamma_t\right) dW_t^F - \beta h \left(N_t \sigma_t^C S_t \gamma_t + \nu^C \delta_t\right) dW_t^C. \end{aligned} \tag{11}$$

Finally, a comparison of equations (11) and (8) reveals that

$$\sigma_t^F = \frac{\nu}{1 + \beta h N_t S_t \gamma_t} \tag{12}$$

$$\sigma_t^C = -\frac{\beta h \nu^C \delta_t}{1 + \beta h N_t S_t \gamma_t}, \tag{13}$$

while the drift has the form

$$\mu_t = \frac{\alpha + \frac{1}{2}(\sigma_t^S)^2 \left(1 - \beta h N_t \psi_t S_t^2\right) - \beta h \left(N_t \chi_t + S_t \gamma_t \nu^C (\rho \sigma_t^F + \sigma_t^C)\right)}{1 + \beta h N_t S_t \gamma_t}. \tag{14}$$

In order to have the dynamics well-defined when $1 + \beta h N_t S_t \gamma_t < \varepsilon$, we control the explosive behavior of the coefficients (12)-(14) by putting a floor equal to ε on the denominator. Hence, for $t \notin \mathcal{T}_\varepsilon$ we impose that

$$\begin{aligned} \sigma_t^F &= \frac{\nu}{\varepsilon} \\ \sigma_t^C &= -\frac{\beta h \nu^C \delta_t}{\varepsilon} \\ \mu_t &= \frac{\alpha + \frac{1}{2}(\sigma_t^S)^2 \left(1 - \beta h N_t \psi_t S_t^2\right) - \beta h \left(N_t \chi_t + S_t \gamma_t \nu^C (\rho \sigma_t^F + \sigma_t^C)\right)}{\varepsilon}, \end{aligned}$$

ensuring that the stock price dynamics are well-defined for all $t \geq 0$. Effectively, we are putting

a limit on the gamma effect by this adjustment. One may interpret this as imposing a behavioral constraint on market makers, whereby they hedge their exposure only partially when the required rebalancing positions become excessively large.

Assuming that we are in the domain where $\beta h N_t S_t \gamma_t > -1$, some intuition on the impact of option hedging can be gained from equations (11)-(13). Focusing on the first diffusive term and noting that for a call option $\gamma_t > 0$, we see that for a negative dealer position in options, $N_t < 0$, the fluctuations arising from shocks to the fundamental price are scaled up via (12). In contrast, when $N_t > 0$ the same shocks to the fundamental price are scaled down. This effect is well documented in a number of papers and has been termed the gamma effect (Baltussen et al. 2021, Barbon and Buraschi 2020, Barbon et al. 2021, Ni et al. 2021). Likewise, focusing on (13), we see that $\sigma_t^C < 0$ when the option delta is positive (call options). Hence, for a positive shock to the dealer's net position in call options, the hedging impact on the price of the underlying is negative. In these scenarios, the dealer has to sell the underlying to hedge the delta of the new position. Similarly, a negative shock to the net position implies that the dealer buys the underlying with resulting positive price pressure. Moreover, the price impact is influenced by the gamma effect and can be either magnified or dampened depending on the sign of the aggregate gamma position, $N_t \gamma_t$.

Some interpretation of the stability condition $\beta h N_t S_t \gamma_t = \beta h N_t S_t \frac{\partial \delta_t}{\partial S_t} > -1$ can be gained from rewriting it in discrete form as

$$\frac{-\beta h N_t (\delta_{t+1} - \delta_t)}{(S_{t+1} - S_t)/S_t} < 1. \tag{15}$$

As the quantity $(\delta_{t+1} - \delta_t)$ is of the same sign as $(S_{t+1} - S_t)$, we note that the sign on the left hand side of the inequality (15) is controlled by the sign of the net option position N_t. Hence, since $\beta \geq 0$, the condition is clearly fulfilled whenever $N_t > 0$. The denominator of (15) equals the simple return over some time step while the numerator equals the log-return impact of the OMM's hedging activities connected to the same time step. Hence, in practice the inequality (15) implies that the hedging impact measured in log-return is smaller than 100% of the simple

return. In theory, (15) can be violated as N_t being a Brownian motion can become arbitrary large. In Section 3.3, we document empirically that the condition has only on a very few instances been violated on the considered sample.

2.2 Inclusion of put options to the market

In this section, we extend the model and add puts to the options market. We let the option positions have dynamics

$$dN_t^C = \nu^C dW_t^C, \qquad dN_t^P = \nu^P dW_t^P, \tag{16}$$

where the increments of $\mathbf{W}_t = \left(W_t^F, W_t^C, W_t^P\right)$ are multivariate normal with covariance matrix

$$d\mathbf{W}_t d\mathbf{W}_t^\top = \begin{pmatrix} 1 & \rho_{FC} & \rho_{FP} \\ \rho_{FC} & 1 & \rho_{CP} \\ \rho_{FP} & \rho_{CP} & 1 \end{pmatrix} dt.$$

We assume a linear price impact as in equation (4) with

$$\mathcal{T}_\varepsilon = \{t \geq 0 \mid 1 + \beta h(N_t^C + N_t^P) S_t \gamma_t \geq \varepsilon\}.$$

Inclusion of puts to the market introduces a risk factor to the stock price dynamics due to the price impact of new put options being hedged by the market maker. Therefore, the extended dynamics take the form

$$dS_t = \mu_t S_t\, dt + \sigma_t^F S_t\, dW_t^F + \sigma_t^C S_t dW_t^C + \sigma_t^P S_t dW_t^P, \tag{17}$$

and setting $\sigma_t^S = \sqrt{\sum_i (\sigma_t^i)^2 + 2\sum_{i \neq j} \rho_{ij} \sigma_t^i \sigma_t^j}$ for $i, j = F, C, P$, the log-price dynamics follows

$$ds_t = \left(\mu_t - \frac{1}{2}(\sigma_t^S)^2\right) dt + \sigma_t^F dW_t^F + \sigma_t^C dW_t^C + \sigma_t^P dW_t^P. \tag{18}$$

We assume that the maturity and the strike price of the call and the put options traded are the same. In this case, we have the connection between their deltas

$$\delta_t^C = 1 + \delta_t^P, \tag{19}$$

and with $\kappa = \chi_t + \mu_t S_t \gamma_t + \frac{1}{2}\psi_t S_t^2 (\sigma_t^S)^2$ the dynamics of the option deltas takes the form

$$d\delta_t^C = d\delta_t^P \approx \kappa dt + \sigma_t^F S_t \gamma_t dW_t^F + \sigma_t^C S_t \gamma_t dW_t^C + \sigma_t^P S_t \gamma_t dW_t^P, \tag{20}$$

where the approximation is due to higher order implied volatility related option Greeks being ignored. The hedging position at time t equals

$$V_t = -h(N_t^C \delta_t^C + N_t^P \delta_t^P) = -h\left((N_t^C + N_t^P)\delta_t^C - N_t^P\right).$$

Hence, the dynamics of the hedge can be found as

$$dV_t = -h\left((N_t^C + N_t^P)d\delta_t^C + \delta_t^C d(N_t^C + N_t^P) + d(N_t^C + N_t^P)d\delta_t^C - dN_t^P\right),$$

which allows us to compute the log-price dynamics using equations (4), (20), and (16)

$$\begin{aligned} ds_t = &\left[\alpha - \beta h(N_t^C + N_t^P)\kappa - \beta h S_t \gamma_t \left(\nu^C \sum_i \sigma_t^i \rho_{iC} + \nu^P \sum_i \sigma_t^i \rho_{iP}\right)\right] dt \\ &+ \left(\nu - \beta h(N_t^C + N_t^P)\sigma_t^F S_t \gamma_t\right) dW_t^F - \beta h\left((N_t^C + N_t^P)\sigma_t^C S_t \gamma_t + \nu^C \delta_t^C\right) dW_t^C \\ &- \beta h\left((N_t^C + N_t^P)\sigma_t^P S_t \gamma_t + \nu^P \delta_t^P\right) dW_t^P. \end{aligned} \tag{21}$$

A comparison of (21) with (18) reveals that when $t \in \mathcal{T}_\varepsilon$ we have that

$$\sigma_t^F = \frac{\nu}{1 + \beta h(N_t^C + N_t^P) S_t \gamma_t} \tag{22}$$

$$\sigma_t^C = -\frac{\beta h \nu^C \delta_t^C}{1 + \beta h(N_t^C + N_t^P) S_t \gamma_t} \tag{23}$$

$$\sigma_t^P = -\frac{\beta h \nu^P \delta_t^P}{1+\beta h (N_t^C + N_t^P) S_t \gamma_t}, \tag{24}$$

while the drift equals

$$\mu_t = \frac{\alpha + \frac{1}{2}(\sigma_t^S)^2 \left(1 - \beta h (N_t^C + N_t^P) \psi_t S_t^2\right) - \beta h \left((N_t^C + N_t^P)\chi_t + S_t \gamma_t \sum_i \sigma_t^i \left(\nu^C \rho_{iC} + \nu^P \rho_{iP}\right)\right)}{1+\beta h (N_t^C + N_t^P) S_t \gamma_t}. \tag{25}$$

Similar to the case when only calls are traded, we adjust the coefficients by putting a floor equal to ε on the denominator in (22)-(25) ensuring that the model is well-defined for all $t \geq 0$.

Focusing on the time points where $\beta h (N_t^C + N_t^P) S_t \gamma_t > -1$, leads to similar interpretations of the equations (22)-(24) as in the case when only call options are traded. Moreover, we notice that a positive shock to the OMM's position in put options leads to a positive impact on the stock price since the OMM needs to buy the underlying asset to match the negative delta of the option.

3 Modeling analysis

We devote this section to analyze the model presented in Section 1. First, Section 3.1 introduces the data used for the analysis. Next, Section 3.2 details the algorithms used to infer the net option position of the OMM throughout the sample period as well as providing descriptive statistics of the inferred times series. The model is estimated in Section 3.3 and, finally, we perform a simulation analysis of the model in Section 3.4.

3.1 Data description

The empirical analysis is conducted using a high frequency data set covering the period from January 2012 to August 2023. Quote and trade data on SPX options is provided by Cboe LiveVol while data on E-mini S&P 500 futures is obtained from Tick Data. SPX options trade on the Chicago board options exchange (Cboe) and the SPX futures on the Chicago Mercantile Exchange (CME). Both the SPX options and the SPX futures trade close to 24 hours a day

during the week. However, we focus our analysis on trades during the regular trading hours (weekdays 9.30-16.15 EST), where most of the trading is executed. The tick-by-tick trade data on SPX options is recorded at millisecond precision, while the quote data is minute-by-minute. For the SPX futures, both trade and quote data is tick-by-tick recorded at millisecond precision. Following the procedure for intraday data filtering proposed in Barndorff-Nielsen et al. (2009), we modify the data accordingly: trades with negative price and quotes with negative bid or ask price are removed. We merge trades or quotes occurring at the same time into the median across the simultaneous values. Non-business days are removed from the sample. Finally, we follow Bangsgaard and Kokholm (2025) and consider for each sample date the SPX futures contract with the shortest time to expiration, unless the time to expiration is less than six days, in which case we roll over to the next maturing contract.

3.2 Inferring the net option position of option market makers

In order to assess the end-of-day hedging demand of the option market maker, we need to infer the net position (or option inventory) at any given time point during the sample period. Baltussen et al. (2021) use the simplifying assumption that the end-user demand is long in put options and short in call options. Coupled with data on the open interest of the option contracts, the assumption allows for the estimation of the option inventory. This assumption originates in the literature on net buying pressure where Bollen and Whaley (2004) and Garleanu et al. (2008) find that market makers in US equity option markets face positive net demand, predominantly negative for calls and positive for puts. More recently, Christoffersen et al. (2018) and Goyenko and Zhang (2019) confirm the same finding on more recent data by measuring order imbalances in option markets. Hence, to some extent the rough assumption of the market maker net position seems empirically justified. By delving into transaction-level data and signing trades using a trade classification algorithm (detailed in the next section), we find some confirmation of the simplifying assumption, in the sense that end-users *generally* buy puts and sell calls. However, the actual inferred dynamics of the net positions are more nuanced than those implied by the simplifying assumption.

3.2.1 Trade classification

For a wide range of research questions, the trade direction of a transaction is relevant information. We devote this section to sketch the classification procedure followed in the present work. The Lee and Ready (1991) (LR) algorithm is often applied due to its simplicity. It uses the quote rule to classify all non-midspread trades, and resorts to the tick rule whenever a trade is directly between the quoted bid and ask price.[2] Numerous classification algorithms have been developed with varying degrees of success (see, e.g., Easley et al. (2016)).

Recently, Grauer et al. (2023) address the limitations of existing trade classification algorithms when applied to option trades, and they propose two modifications to the existing algorithms. First, they hypothesize that trades with size equal to either the quoted bid or ask size are often misclassified by the quote rule due to the use of limit orders placed by (so-called) sophisticated customers. As a solution, the *size rule* states that trades with size equal to the quoted bid size are end-user buys, and trades with size equal to the ask size are customer sells.

Trades executed exactly between the bid and ask price are usually classified using the tick rule, which can be reasonable accurate when signing stock trades (Easley et al. 2016). However, the application of the tick rule to option trade data is more questionable due to liquidity considerations and no-arbitrage connections across different option prices. To tackle this, the *depth rule* hypothesizes that a larger quoted bid or ask size (i.e., a higher depth) indicates higher liquidity. Thus, midspread trades are classified as end-user buys when the ask size exceeds the bid size, and end-user sells in the opposite case.

In specific, we will employ the two new rules together with the quote rule (labeled the GSU trade algorithm), and apply the standard quote rule as a benchmark, which is a more conservative approach compared to the LR algorithm, as it leaves midspread trades unclassified. As expected, the results using the different classification algorithms are comparable with similar coefficients and significance. To our knowledge, these modifications have not yet been utilized for option trade classification in empirical studies on the interlink between the stock and the

[2] *The quote rule*: Trades with price above (below) the midspread are classified as buys (sells). Midspread trades are not classified. *The tick rule*: Trades with price above (below) the closest different trade price of a previous trade are classified as buys (sells).

option markets. In Grauer et al. (2023), the improved classification accuracy is mainly due to the size rule, which is based on the quoted sizes. In our data, only 3.7% of the trading volume is classified using the size rule as opposed to 14.0% in their entire option sample. Instead, most of the classification differences to the quote rule are driven by the *depth rule*, as 14.6% of the volume in our sample consists of midspread trades.

Once the net option trading is known for all time points, a time series for the market maker's net position in each individual option can be constructed. The initial option net position on the first sample day is approximated by multiplying the open interest on the day with the empirical probability of being short or long in an option, for each option type. While this approach may be somewhat ad hoc, its impact on the final conclusions is expected to be minimal, given that options on the first sample date will expire early in the sample period.

The descriptive statistics for the inferred net positions in Table 1 highlight the similarities of the GSU and quote rule trade classification algorithms, where the quantiles, mean, and standard deviations are equivalent in magnitude, across both call and put options. Further, we also see that the market maker's net position in put options tends to be negative, while the call option position tends to be positive although of smaller magnitude.

	Obs	Mean	Std. dev.	Min	0.05	0.25	0.50	0.75	0.95	Max
Panel A: GSU trade classification algorithm										
$N^C_{t,1min}$	1,179,495	86.528	275.478	-1142.899	-368.036	-84.913	109.195	257.310	525.601	1012.399
$N^P_{t,1min}$	1,179,495	-524.062	503.729	-2251.934	-1426.568	-830.145	-503.240	-163.918	249.265	752.783
$N^C_{t,daily}$	2923	85.262	279.163	-1105.702	-378.011	-88.059	107.156	258.741	530.687	991.602
$N^P_{t,daily}$	2923	-536.501	511.088	-2204.955	-1461.564	-844.384	-520.481	-162.395	250.206	748.912
Panel B: Quote rule trade classification algorithm										
$N^C_{t,1min}$	1,179,495	83.600	274.773	-1036.963	-377.226	-102.881	93.448	266.271	534.511	979.827
$N^P_{t,1min}$	1,179,495	-508.796	509.097	-2285.909	-1400.114	-834.535	-486.575	-132.447	297.012	704.433
$N^C_{t,daily}$	2923	81.790	279.173	-1007.055	-384.055	-106.405	91.416	269.124	538.759	961.581
$N^P_{t,daily}$	2923	-521.450	517.590	-2223.810	-1428.422	-857.738	-503.367	-137.401	288.561	701.269

Table 1: Descriptive statistics for the inferred market maker option inventory. All values are in thousands. $N_{t,1min}$ is sampled at a one minute frequency, whereas $N_{t,daily}$ is sampled daily by market close.

Figure 2 depicts the daily time series of the inferred net position in calls and puts for the OMM using the GSU trade classification. Towards the end of the sample period, the market maker net position appears more balanced in both option types. The massive entrance of retail

investors to the options market can explain the data as these investors engage more in speculative trading. In particular, Bryzgalova et al. (2023) document that retail investor trading recently reached over 60% of the total market volume in options in the US. This observation also indicates that the assumption of the market maker being net short in put options and long in call options had more merit before the massive entrance of retail traders to the market.

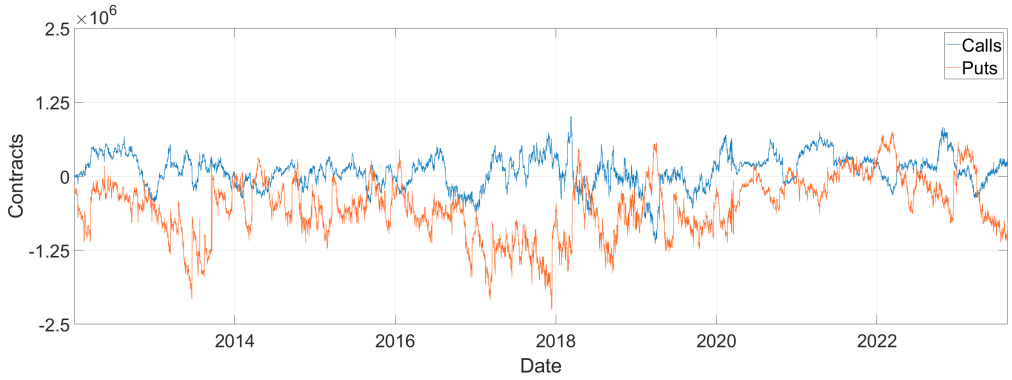

Figure 2: Market maker inventory for each option type, inferred using the GSU trade classification algorithm. End-users are typically buying puts and selling calls. Compared to the earlier years, we see indications of the options trading becoming more balanced towards the end of the sample.

3.3 Model estimation

We estimate the model with the time series data on the SPX futures and the data on the SPX options. Using our inferred time series for market maker option inventory N_t^C, N_t^P alongside the observed series on the futures price S_t, we proceed to estimate the model parameters. Notably, the model does not permit a direct identification of the components β and h as the two always appear as the product βh. Consequently, to obtain individual estimates for h and β, one must resort to estimating either parameter outside the model framework. Hence, to ease the notation going forward, we assume $h = 1$ and report estimates of β.

Table 1 reveals similar descriptives of the two inferred times series of the option positions. Here, we focus the estimation on the times series of the net option position based on the GSU algorithm. We get similar results if we estimate the model based on the quote rule trade classification algorithm. First, we estimate the linear price impact, $\beta = 1.900 \cdot 10^{-8}$ by regressing

daily log differences in the SPX futures value against changes in the net delta position. Moreover, we estimate the volatilities on the option net positions $\nu^C = 9.514 \cdot 10^5$, $\nu^P = 1.698 \cdot 10^6$ (annualized) and correlations $(\rho_{FC}, \rho_{FP}, \rho_{CP}) = (-0.182, 0.211, -0.222)$. Note that S_t and N_t^P are positively correlated, such that when the underlying drops in value, end-users are buying puts (OMM is selling). In contrast, end-users tend to sell calls in a market decline. Hence, in both cases the OMM sells the underlying putting additional negative price pressure on the underlying security. The estimated values are collected in Table 2.

β	ν^C	ν^P	ρ_{FC}	ρ_{FP}	ρ_{CP}
$1.900 \cdot 10^{-8}$	$9.514 \cdot 10^5$	$1.698 \cdot 10^6$	-0.182	0.211	-0.222

Table 2: Estimation of model parameters. The correlations involving F_t are estimated using S_t as substitute, since F_t by definition is unobservable.

Figure 3 reveals that in times with very unbalanced market maker option inventory (and with sizable positions in options with large gammas), the volatilities connected to the different stochastic drivers are roughly 20% away from its fundamental value due to the gamma effect. Recall that when $\beta h(N_t^C + N_t^P) S_t \gamma_t > 0$, the volatility is dampened and when $\beta h(N_t^C + N_t^P) S_t \gamma_t < 0$ the volatility is elevated compared to the fundamental value. Likewise, the drift in (25) is impacted by the gamma position of the OMM. In any case, the time series indicate that empirically the inequality $\beta h(N_t^C + N_t^P) S_t \gamma_t > -1$ is essentially never violated.

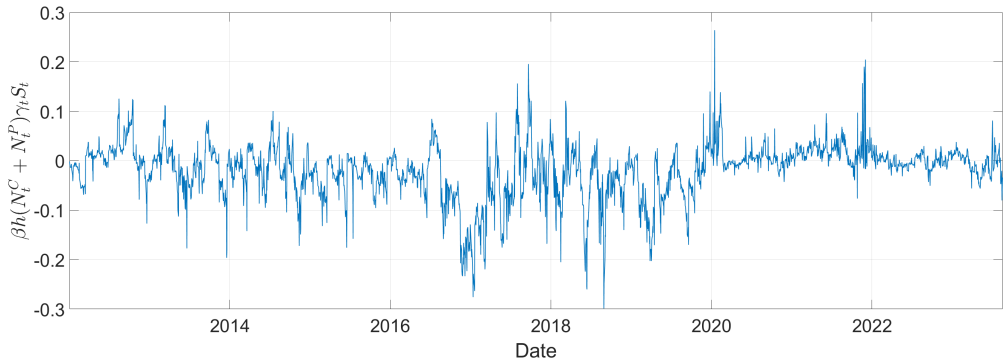

Figure 3: Time series of the end-of-day value of $\beta h(N_t^C + N_t^P) S_t \gamma_t$.

However, when repeating the exercise at a 15-minute frequency, there is a single case out of the 82,000 observations where the value drops below -1 (see Figure 4). The majority of the large

values of $|\beta h(N_t^C + N_t^P)S_t\gamma_t|$ are towards the end of the day, when the gamma is increasingly sensitive towards short-term options and end-users are adjusting their option portfolio before market close.

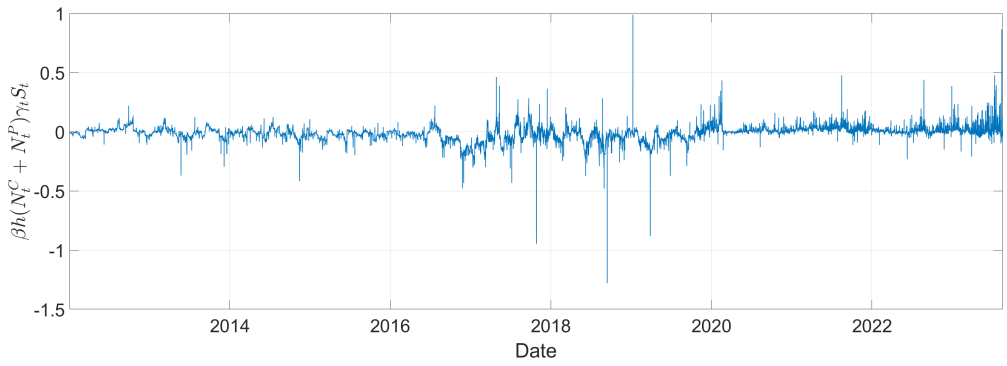

Figure 4: Time series of the value of $\beta h(N_t^C + N_t^P)S_t\gamma_t$ on a 15-minute frequency.

To retrieve an estimate of ν, we consider the non-linear regression model

$$\sigma_t^S = \sqrt{\sum_i (\sigma_t^i)^2 + 2\sum_{i\neq j} \rho_{ij}\sigma_t^i\sigma_t^j}, \tag{26}$$

for $i, j = F, C, P$, and the expressions for σ_t^F, σ_t^C, and σ_t^P given in (22), (23), and (24). In the implementation, we swap $(N_t^C + N_t^P)\gamma_t$ with $\sum_i (N_{t,i}^C + N_{t,i}^P)\gamma_{t,i}$, such that the net gamma exposure adds the gamma exposure of all outstanding option positions i. Moreover, we approximate σ_t^S with the VIX, which provides an estimate of the 30-day expected volatility of S_t. Hence, given the parameter estimates reported in the previous section, the only unknown is ν.

Time series for δ_t^C and δ_t^P for the traded option pair introduced in the model setup are needed for the estimation procedure. We use the open interest of the options traded to compute the strike and the maturity of a representative option pair. In specific, for each t we compute a representative strike, $K_t^R = \sum_{i\in\text{options}} w_t^i K^i$, and maturity, $\tau_t^R = \sum_{i\in\text{options}} w_t^i \tau^i$, where the weights are determined as $w_t^i = \frac{OI_t^i}{\sum_{i\in\text{options}} OI_t^i}$ and OI_t^i is the open interest of the i'th option at time t. For each t we then do bilinear interpolation in the (K, τ)-space with the closest options to estimate δ_t^C and δ_t^P. This procedure also ensures that the relationship $\delta_t^C = 1 + \delta_t^P$ holds. The non-linear regression from (26) yields the estimate $\hat{\nu} = 0.1682$, which allows us to examine the behavior

of σ_t^S as a function of the market maker's net gamma position.

Figure 5 depicts the inverse relationship between the net gamma position of the market maker and the volatility of the underlying asset, S_t. In particular, the volatility blows up when the gamma position gets more and more negative. When the market maker holds a balanced option inventory, that is, $N_t^C + N_t^P = 0$, it does not imply that $\sigma_t^S = \nu$, as opposed to the volatility term related to the pure gamma effect, σ_t^F. This is due to the additional volatility terms arising from the stochasticity of N_t^C and N_t^P, representing changes to the option inventory rather than the option gamma. In this case, we have $\sigma_t^S = 0.1743$ and the difference $\sigma_t^S - \nu = 0.61\%$ arises due to the price impact incurred when the OMM hedges changes to the option inventory. Finally, on the left wing of σ_t^S, we observe the cap imposed on the volatility terms when the gamma position of the OMM becomes too unbalanced to the negative side.

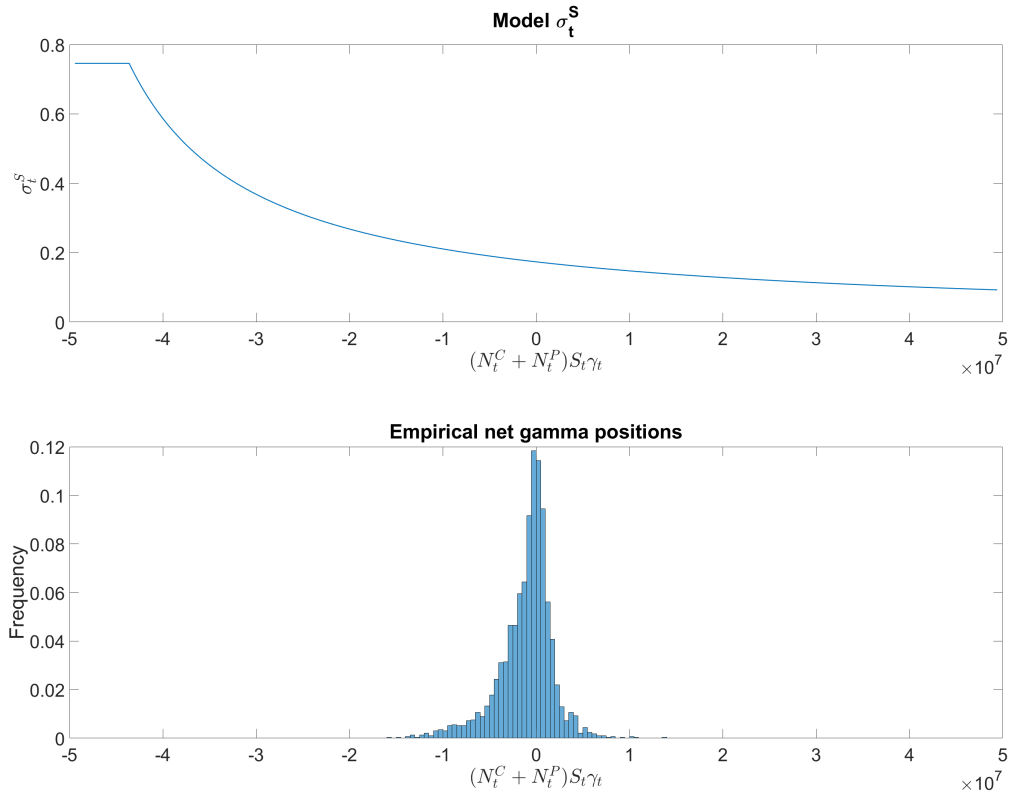

Figure 5: Plot of the model volatility of the observed stock index, σ_t^S, as a function of the net gamma exposure with $\delta^C = 0.5$ and $\varepsilon = 0.25$. Comparing with the empirical distribution of end-of-day market maker net gamma positions, the volatility of S_t lies in the range of 15% to 22%.

3.4 Simulation analysis

To analyze how our model incorporates the market maker's hedging effects on the return of the underlying asset, we simulate the relevant processes using Euler discretizations. We use the parameters estimated in the previous section and put $S_0 = K = 1{,}000$, $\tau = 1$, and $\alpha = -\frac{1}{2}\nu^2$. In the simulation, we set $\varepsilon = 0.25$ to prevent coefficient blow-ups. In practice, the floor on the denominator of equations (22)-(25) is never binding when using the estimated parameters reported in Table 2.

Figure 6 depicts simulated sample paths of our model. A few observations are evident from inspection of Figure 6. While S_t and F_t move closely together, the sample path of the observed stock price is slightly more volatile. From the lower panel of Figure 6, we observe that the volatility of S_t is stochastic, which arises from σ_t^F, σ_t^C, and σ_t^P all being stochastic. The stochasticity of σ_t^F arises entirely from the gamma effect while the stochasticity of σ_t^C and σ_t^P arise from the dynamics of the option delta amplified/dampened via the gamma effect. Also, we observe that $\sigma_t^S > \sigma_t^F$ highlighting that neglecting to take into account the fluctuations in the option positions will underestimate the volatility of the stock price. σ_t^F fluctuates around the constant volatility, ν, of the fundamental asset. Note that $\sigma_t^F > \nu$ when the market maker is in a short gamma position, and $\sigma_t^F < \nu$ when the position is long. The sign of the overall gamma position can be inferred by adding the time series of N_t^C and N_t^P depicted in the upper right corner of Figure 6. Finally, we see that σ_t^C and σ_t^P are intimately connected due to the close connection between the deltas of the call and put options formalized by equation (19).

To quantify the downside of the friction introduced by the market maker's delta hedging activities, we compute both the Value-at-Risk (VaR) and Expected Shortfall (ES) of the log-returns of the observable price S_t, the fundamental value F_t, and the difference between the two. Furthermore, by varying the strike, K, of the options, we are able to analyze the hedging impact for different values of the initial delta of the option. We simulate 1,000,000 independent realizations of our model on a yearly horizon and report the outcome in Table 3. Considering the case $\delta_0^C = \delta_0^P = 0.5$, the model yields a Value-at-Risk of 1.75% for the fundamental price, while it is 1.86% for the observable price. This means that the hedging activities imply that the

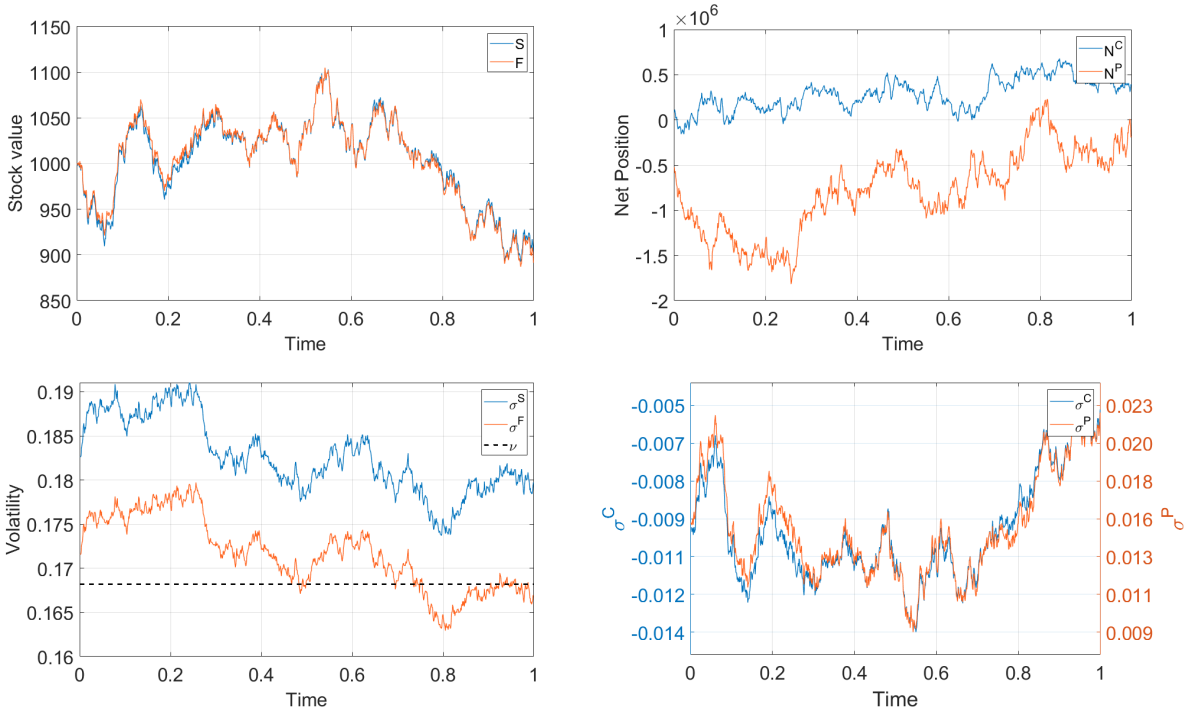

Figure 6: Simulated paths of relevant processes with the specified parameters.

loss in stock value is 0.11 percentage points worse at the 5% level. The conclusion for the ES values is the same with slightly larger values.

δ_0^C	0.1	0.2	0.3	0.4	0.5	0.6	0.7	0.8	0.9
S_{VaR}	1.861	1.861	1.860	1.857	1.855	1.852	1.847	1.841	1.832
$S_{VaR} - F_{VaR}$	0.112	0.111	0.110	0.108	0.105	0.102	0.097	0.091	0.082
S_{ES}	2.342	2.341	2.340	2.337	2.334	2.330	2.324	2.316	2.304
$S_{ES} - F_{ES}$	0.148	0.147	0.146	0.143	0.139	0.135	0.129	0.122	0.110

Table 3: Daily Value-at-Risk and Expected Shortfall based on daily log-returns for the model with hedging friction and the one without at the 5% level. All values are in %. For the fundamental value F_t, we analytically calculate for daily values $VaR = 1.75\%$ and $ES = 2.19\%$ at the 5% level.

The monotonic increase (absolutely) of S_{VaR} and S_{ES} as $\delta^C \to 0$, is an outcome of the model construction in combination with the model parameters. As the call option delta approaches zero, the corresponding put option delta, $\delta^P = \delta^C - 1$, goes towards -1, and both the VaR and ES of S_t increase in absolute sense. Empirically $\nu^P > \nu^C$ which from equations (23)-(24) imply that for the same level of delta, put options introduce more volatility in the price dynamics in comparison to call options, due to the more volatile trading of the former.

The differences on a daily basis are minimal, a result anticipated given the parameters estimated across the entire sample. However, as detailed in Section 4.4, the significance of hedging becomes more pronounced during periods of extreme absolute returns. Such instances are usually the primary concern for market participants. Hence, repeating the simulation study using parameters estimated in a more volatile market environment would yield a clearer understanding of the impacts. Analyzing the 10% most volatile trading days in our sample, we obtain the parameter estimates $\beta = 1.008 \cdot 10^{-7}$, $\nu^C = 9.823 \cdot 10^5$, $\nu^P = 1.680 \cdot 10^6$, and $(\rho_{FC}, \rho_{FP}, \rho_{CP}) = (-0.342, 0.355, -0.277)$. Notably, the impact coefficient β has increased by a factor 5, suggesting a significantly increased hedging impact on returns. In these extreme instances, the VaR of daily returns increase by roughly óne percentage point, as implied by the OMM delta hedging approach.

Additionally, we are interested in delving into the relationship between the net gamma exposure and changes in net delta and their impact on stock price dynamics through the market maker's hedging activities. For clarity, we focus on the 5% quantile of the return series r_t^F. This limits our scope to instances when an already negative market movement in the underlying is intensified or dampened by the market maker's delta hedging. From a regulatory perspective on financial stability, the case of intensified negative returns raises most concerns.

In the lower panel of Figure 7, we see that a short gamma position is not always required for large hedging induced negative returns to be realized. Likewise, there are instances with large, negative gamma positions, but the return difference is still negligible. Conversely, there are also cases of positive gamma, where the market maker is positioned to have a dampening effect on the negative return, but the overall effects imply more negative returns. We can interpret this as days, where end-users trade options in a way that forces the market maker to delta hedge these by selling the underlying (and in a magnitude larger than the negative delta change implied by the gamma position).

By merging the plots of Figure 7, we are able to examine the interplay between the gamma exposure and inventory effect (end-user option trading) more closely. Figure 8 reveals that the impact of the market maker's option hedging is not adequately explained by the OMM's

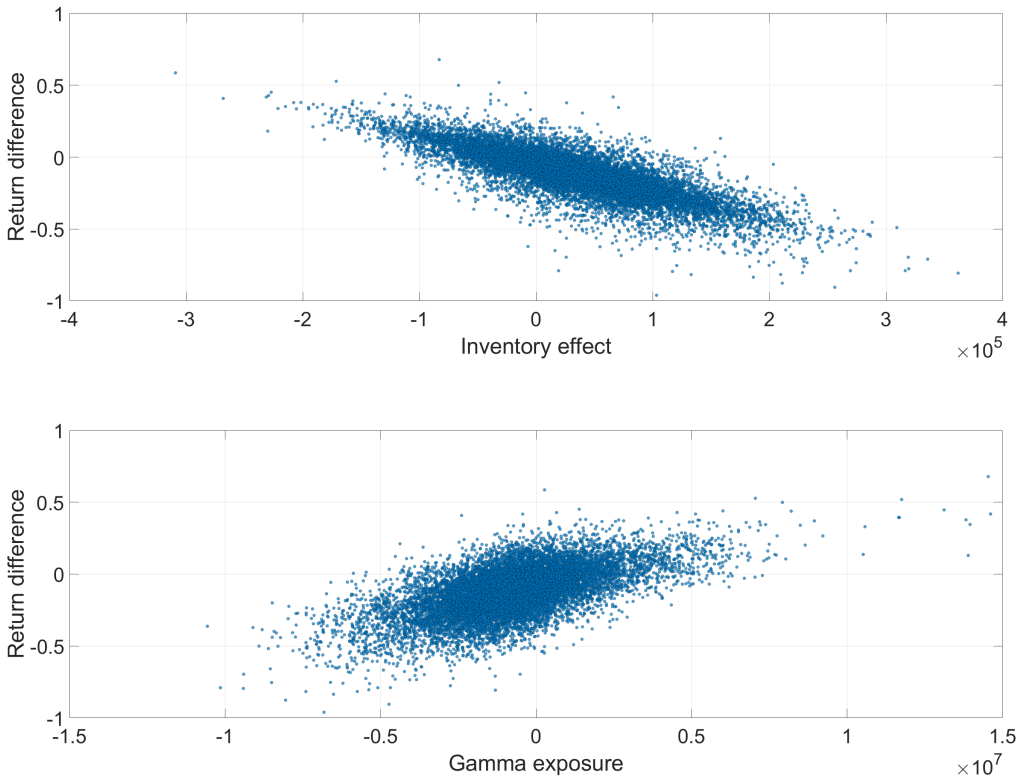

Figure 7: Daily values of $r_t^S - r_t^F$ in % plotted against the inventory effect and gamma exposure. In the first plot, we observe that significant negative returns are associated with a large positive change in the option (delta) inventory, forcing the market maker to sell the underlying asset. Similarly, in the lower plot, a large negative gamma position magnifies market dips. The cloud of points is slightly shifted to the left, since negative gamma imbalance is strongly related to the large negative return differences.

gamma exposure alone. In general, the color change when moving downward in the graph highlights the perfect storm of considerable negative gamma exposure combined with a big positive change to the option (delta) inventory, where both effects force the market maker to sell the underlying in an already falling market. A similar analysis could be conducted with, for instance, the largest values of r_t^F, which would then focus on cases when positive stock returns are either dampened or amplified.

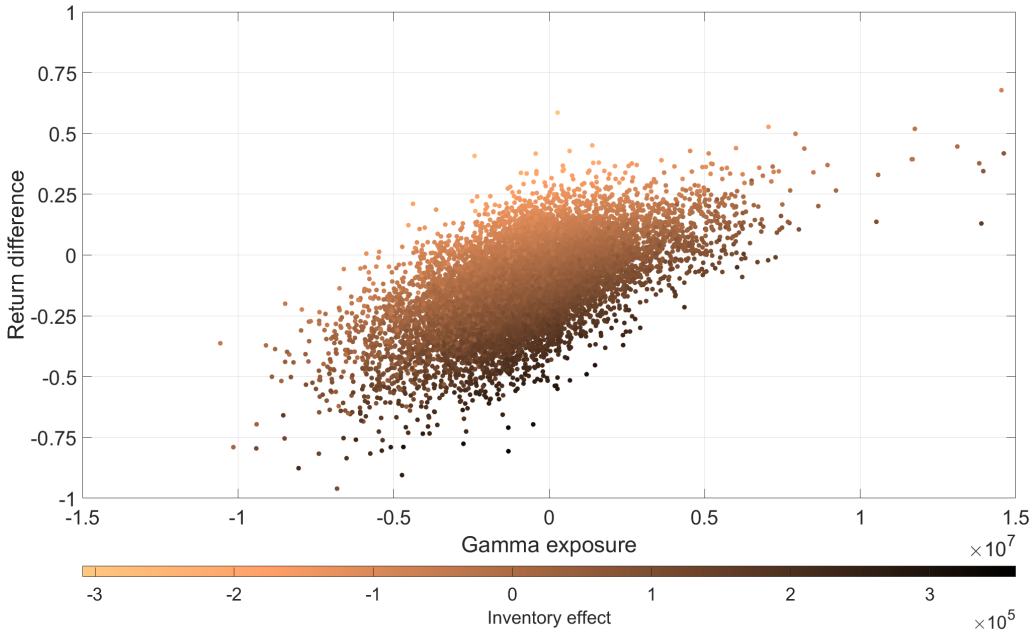

Figure 8: Daily values of $r_t^S - r_t^F$ in % plotted against gamma exposure while the color code allows us to simultaneously consider the inventory effect.

4 Predicting stock returns based on the hedging demand

To detect a possible hedging price pressure, we need to identify an asset which the market makers use to hedge their option exposure. In the case of SPX options, the most natural choice is the SPX futures as they are traded products designed to track the underlying SPX index. In addition, an investor/hedger can easily form both long and short positions in futures, in contrast to other funded products such as ETFs tracking the SPX index where short-selling constraints might be in place. For these reasons, we choose the SPX futures to look for an hedging impact.

In Section 4.1, we consider a regression model where we regress the end-of-day SPX futures returns against the estimated time series of the daily change in the net option position. Section 4.2 considers a decomposition of the net delta position into a component reflecting the gamma effect and a component reflecting the change in the option inventory, and the end-of-day SPX futures returns time series is regressed on the two resulting time series. Next, in Section 4.3 we repeat the analysis of Section 4.1 but conditioned on the realization of a large SPX futures return. Finally, Section 4.4 is devoted to study the hedging impact on an intradaily frequency.

4.1 End-of-day SPX futures returns and net option delta changes

We will analyze to what extent the hedging demand of the OMM can explain SPX futures returns in the window 15.45-16.15, a time slot we posit for the market maker's end-of-day delta hedging activities. We choose a relatively wide time window, as it is challenging to pin down exactly when market makers are hedging their exposure. A few considerations lead us to look for an end-of-the-day impact. First, the OMM may choose to postpone the hedge until the end of the day to allow option demand to balance out throughout the day. However, in order to protect the OMM against overnight risk, the option exposure should be hedged by the market close. As the SPX options trade extensively until the market close at 16.15, it makes sense to postpone hedging until the suggested time slot (see upper panel of Figure 9). Second, Hong and Wang (2000) show that it is optimal for market makers to close their delta hedges before market close, as holding unhedged option positions overnight triggers additional capital requirements. Third, by postponing the hedge, the OMM can benefit from the relatively higher market depth at the end of the day (Baltussen et al. 2021). Indeed, Figure 9 shows that apart from the beginning of the day, the interval 15.45-16.15 has the most trading volume both in SPX options and SPX futures.

Inspired by Bangsgaard and Kokholm (2025), we include a number of control variables in the regressions. To capture potential momentum or reversal effects leading up to the rebalancing window, we include the SPX futures return in the same time slot as the net delta change is measured, $r_{t-1,16.15-t,15.45}$. We also include the trading volume during the day until 15.45 for

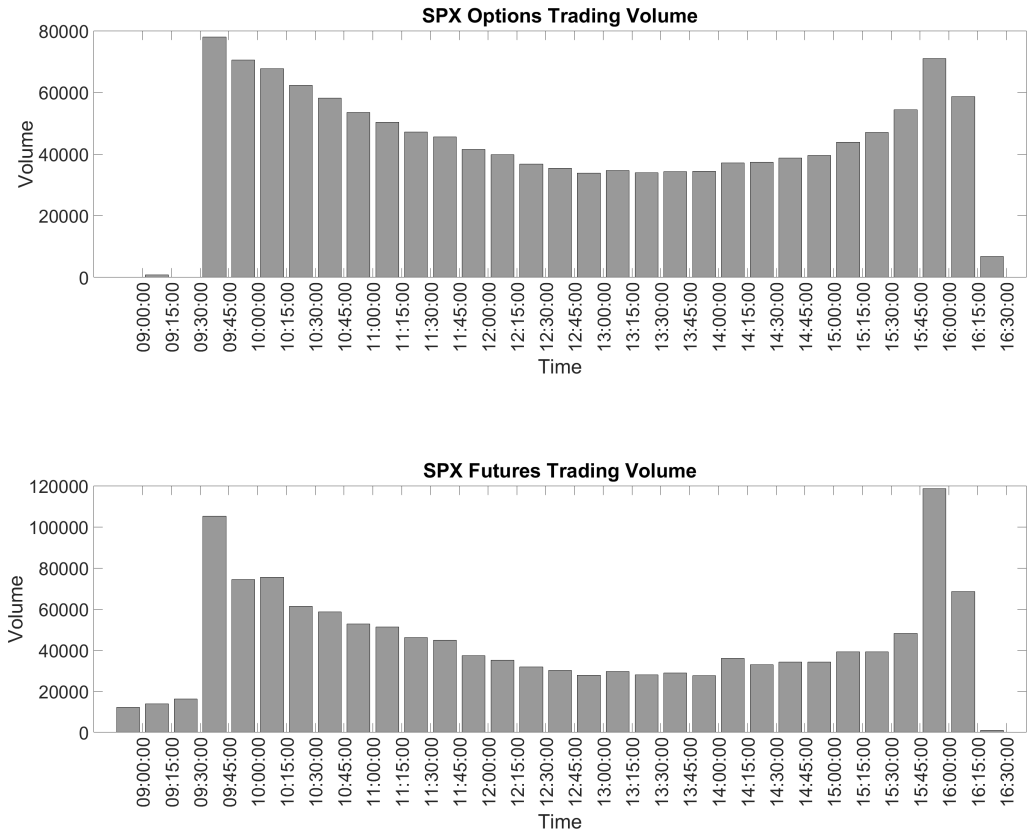

Figure 9: The first two plots are average intraday trading volume in S&P 500 index options and S&P 500 E-Mini futures, respectively. The average trading volume is calculated per 15-minute time interval using the entire data sample, but excluding days when the exchange closed early.

both the SPX futures, $Vol^{ES}_{t,9.30-15.45}$, and the options, $Vol^{SPX}_{t,9.30-15.45}$, respectively. In addition, we include the realized volatility of the SPX futures, $RV_{t,9.30-15.45}$, computed as the square root of the sum of squared 1-minute log returns.

To begin, we do not disentangle the impact of the gamma effect and the hedging impact of changes to the option inventory. Hence, we define the time-t aggregate hedging needs of the OMM as $\Delta_t := \sum_i N^i_t \cdot \delta^i_t$, and consider the regression model

$$r_{t,15.45-16.15} = \alpha + \beta(\Delta_{t,15.45} - \Delta_{t-1,16.15}) + u_t, \tag{27}$$

where $\Delta_{t,15.45} - \Delta_{t-1,16.15}$ is the required delta hedge size at time 15.45 on day t after the previous rebalancing done at 16.15 on day $t-1$. A negative β is consistent with the hedging mechanisms, namely that the market maker buys the underlying when negative delta is accumulated and sells the underlying to offset a positive delta change.

The figures reported in Table 4 show that the market maker's hedging demand negatively predicts the end-of-day return in SPX futures. The coefficient on the primary predictor, $\Delta_{t,15.45} - \Delta_{t-1,16.15}$, is consistently negative and highly significant across all regression models. This suggests a robust relationship between the market maker's hedging demand and the end-of-day returns of SPX futures. The persistence of this effect, despite the introduction of various control variables, underscores its significance. In summary, Table 4 supports the hypothesis that the market maker's hedging demand predicts end-of-day returns for SPX futures.

4.1.1 Triple witching days

The phenomenon of "triple witching" (the simultaneous expiration of stock index futures, stock index options and single-stock options) occurs four times a year, on the third Friday of the last month of each quarter. Early evidence of unusual market activity on these days is reported by Stoll and Whaley (1987). The general finding in this literature is that triple witching days are associated with elevated trading volume and volatility, while the impact on returns is less consistent (Xu 2014).

$r_{t,15.45-16.15}$	(1)	(2)	(3)	(4)	(5)
$\Delta_{t,15.45}$ - $\Delta_{t-1,16.15}$	-0.097*** (-3.459)	-0.090*** (-3.018)	-0.094*** (-3.200)	-0.093*** (-2.796)	-0.089*** (-2.912)
$r_{t-1,16.15-t,15.45}$		0.053 (1.124)			0.038 (0.818)
$Vol^{SPX}_{t,9.30-15.45}$			0.023 (1.013)		0.027 (1.233)
$Vol^{ES}_{t,9.30-15.45}$			-0.070* (-1.850)		-0.047 (-1.267)
$RV_{t,9.30-15.45}$				-0.054 (-1.321)	-0.025 (-0.595)
Adj. R^2 (%)	0.91	1.15	1.29	1.17	1.41
No. of Obs	2917	2917	2917	2917	2917

Table 4: SPX futures return in the hedging window. The table reports regression results for the model in (27). All variables are standardized. Newey-West t-statistics are presented in parentheses, and ***, **, *, indicates 1%, 5% and 10% significance, respectively.

In our setting, triple witching days are relevant because they may amplify option market maker hedging flows, either through hedging of new positions or elevated end-of-day rebalancing pressure. However, when we include a dummy variable for triple witching days in the regression model, the coefficient is statistically insignificant (Table 5). This indicates that, at least in the narrow hedging window we study, these days do not systematically generate predictable SPX futures return.

There are several reasons, why this might be the case. First, market participants are fully aware of these quarterly expiration dates. Hence, market makers can spread out their rolling over and unwinding activities over several days, limiting concentrated order flow at the end of the expiration day. Second, while trading volume and volatility may increase, this does not necessarily imply a directional return effect. Lastly, the number of triple witching dates in the sample is small relative to the total number of observations. So, unless the return effect is very large, any coefficient estimate will be imprecise.

4.2 Decomposition of the net delta position

Typically the gamma exposure of OMMs is the object of analysis when the impact of option hedging is studied (Baltussen et al. 2021, Barbon and Buraschi 2020). In particular, a short net

$r_{t,15.45-16.15}$	(1)	(2)	(3)	(4)	(5)	(6)
$\Delta_{t,15.45}$ - $\Delta_{t-1,16.15}$	-0.097*** (-3.459)	-0.090*** (-3.018)	-0.094*** (-3.200)	-0.093*** (-2.796)	-0.091*** (-2.780)	-0.081** (-2.335)
$r_{t-1,16.15-t,15.45}$		0.053 (1.124)				0.039 (0.829)
$Vol^{SPX}_{t,9.30-15.45}$			0.023 (1.013)			0.027 (1.221)
$Vol^{ES}_{t,9.30-15.45}$			-0.070* (-1.850)			-0.047 (-1.262)
$RV_{t,9.30-15.45}$				-0.054 (-1.321)		-0.025 (-0.598)
Triple witching					-0.118 (-0.548)	-0.136 (-0.665)
Adj. R^2 (%)	0.91	1.15	1.29	1.17	0.90	1.40
N	2917	2917	2917	2917	2917	2917

Table 5: SPX futures return in the hedging window. The table reports regression results for the model in (27) including dummy variables for FOMC meetings and Triple Witching Days. All continuous variables are standardized. Newey-West t-statistics are presented in parentheses, and ***, **, *, indicates 1%, 5% and 10% significance, respectively.

gamma exposure in an already falling market, effectively creates a negative feedback loop. To quantify this in a regression model, the product of the market maker's aggregate gamma position and the return up until the beginning of the hedging window, $\Gamma_{t-1,16.15} \cdot r_{t-1,16.15-t,15.45}$, is used as independent variable. Consequently, the hedging of changes to the option inventory is ignored in these studies. To take this into account, we consider the decomposition

$$\Delta_t - \Delta_{t-1} = \delta_t(N_t - N_{t-1}) + N_{t-1}(\delta_t - \delta_{t-1}),$$

where the first term has the interpretation of hedging of changes to the notional of the option positions, while the second term captures the gamma effect, namely, the rebalancing due to the change in delta of existing option positions from time $t-1$ to time t. Figure 10 provides a visual representation of the two components (the gamma and option inventory effect) of the net delta effect. In the initial segment of the sample, the inventory impact is primarily slightly positive, which loosely speaking aligns with end-users buying puts or selling calls. Moreover, the spikes caused by expiring options are less pronounced in the final years of the sample period due to two main factors. First, the market maker's net position tends to be more balanced, reducing

the influence of large expiring option positions. Second, the introduction of options with varied expiration dates has diminished the reliance on options expiring on the 3rd Friday, which was the primary driver of the spikes.

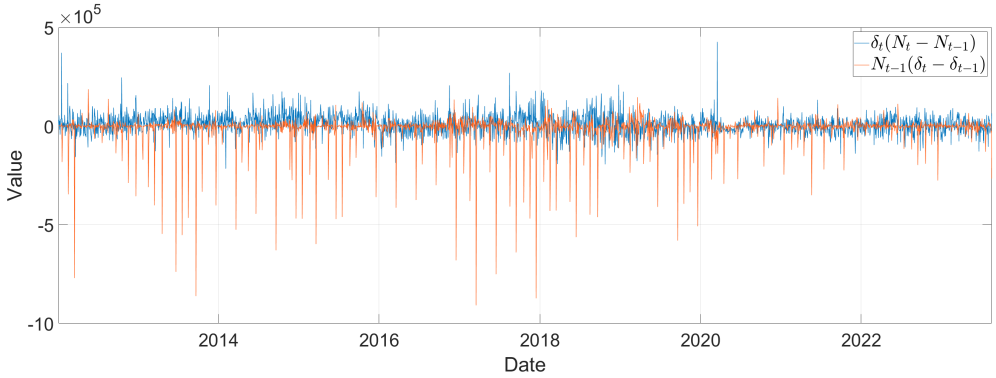

Figure 10: Daily values of the two components of the net delta change. By construction the expiring options appear in the gamma effect, which is visible in the spikes.

With the decomposed net delta, our regression model has the form

$$r_{t,15.45-16.15} = \alpha + \beta_1 \cdot \delta_{t,15.45}(N_{t,15.45} - N_{t-1,16.15}) + \beta_2 \cdot N_{t-1,16.15}(\delta_{t,15.45} - \delta_{t-1,16.15}) + u_t. \tag{28}$$

First, we see that the size and significance of the effects appear robust towards varying the control variables. In the full regression model in column (7), we see that especially the gamma effect is highly statistically significant, whereas the hedging effect of shocks to the market maker option inventory hovers around the 5% significance level. The finding is novel, and the setting departs from the typical setup where only the effect of rebalancing existing positions is included. As opposed to focusing on the gamma effect, $N_{t-1,16.15}(\delta_{t,15.45} - \delta_{t-1,16.15})$, alone, it highlights the importance of including changes to the OMM's option inventory, $\delta_{t,15.45}(N_{t,15.45} - N_{t-1,16.15})$, if one wishes to capture the full impact of hedging activities.

The empirical results reveal that $\beta_1 \neq \beta_2$ (confirmed in an unstandardized regression) suggesting that the hedging impact depends on the origin of the hedging demand. The timing of the OMM's hedging activities can serve as an explanation for this seemingly unintuitive result. For instance, if the OMM chooses to hedge some of the delta exposure arising from changes to the

$r_{t,15.45-16.15}$	(1)	(2)	(3)	(4)	(5)	(6)	(7)
$\delta_{t,15.45}(N_{t,15.45} - N_{t-1,16.15})$	-0.083**		-0.087**	-0.081**	-0.083**	-0.080*	-0.079*
	(-2.204)		(-2.283)	(-2.056)	(-2.023)	(-1.883)	(-1.880)
$N_{t-1,16.15}(\delta_{t,15.45} - \delta_{t-1,16.15})$		-0.056***	-0.061***	-0.056***	-0.061***	-0.061***	-0.058***
		(-3.109)	(-3.326)	(-3.194)	(-3.346)	(-3.092)	(-3.231)
$r_{t-1,16.15-t,15.45}$				0.051			0.038
				(1.079)			(0.799)
$Vol^{SPX}_{t,9.30-15.45}$					0.027		0.031
					(1.088)		(1.263)
$Vol^{ES}_{t,9.30-15.45}$					-0.069*		-0.047
					(-1.784)		(-1.250)
$RV_{t,9.30-15.45}$						-0.050	-0.023
						(-1.205)	(-0.553)
Adj. R^2 (%)	0.66	0.28	1.00	1.23	1.36	1.22	1.47
No. of Obs	2917	2917	2917	2917	2917	2917	2917

Table 6: The table reports regression results for the model in (28) with the decomposed change in net delta from 16.15 on day $t-1$ to 15.45 on day t. All variables are standardized. Newey-West t-statistics are presented in parentheses, and ***, **, * indicates 1%, 5%, and 10% significance, respectively.

option inventory during the day, we are effectively measuring the end-of-day hedging demand due to inventory changes inaccurately, and the β-coefficients of the two hedging components will differ when we run the regression. We explore this further in Section 4.4. In addition, the time series for the gamma effect exhibits pronounced spikes compared to the inventory effect (See Figure 10) These spikes will inflate the variance of the regressor and, if they are not systematically related to the SPX futures returns (as suggested in Secion 4.1), this will shrink the estimated coefficient, β_2, in absolute value.

4.3 Large absolute end-of-day returns

The SPX futures market is likely sufficiently liquid to absorb smaller demands with limited price impact as a result. However, a sufficiently large demand may cause a more significant price impact (Almgren et al. 2005, Bouchaud et al. 2009, Lillo et al. 2003, Patzelt and Bouchaud 2018). Hence, we devote this section to study the impact conditioned on the realization of a large market movement, positive or negative. In specific, we consider the subsample defined by the absolute end-of-day returns above the 90% quantile, i.e. the sample that satisfies

$|r_{t,15.45-16.15}| > 0.34\%$.[3] By repeating the regression in (27), we examine the predictability of the end-of-day SPX futures return on the reduced sample in Table 7.

$r_{t,15.45-16.15}$	(1)	(2)	(3)	(4)	(5)
$\Delta_{t,15.45}$ - $\Delta_{t-1,16.15}$	-0.299*** (-3.839)	-0.290*** (-3.198)	-0.311*** (-3.877)	-0.300*** (-3.422)	-0.302*** (-3.352)
$r_{t-1,16.15-t,15.45}$		0.061 (0.582)			0.066 (0.597)
$Vol^{SPX}_{t,9.30-15.45}$			0.091 (1.308)		0.087 (1.192)
$Vol^{ES}_{t,9.30-15.45}$			-0.071 (-0.703)		-0.072 (-0.748)
$RV_{t,9.30-15.45}$				0.021 (0.375)	0.040 (0.582)
Adj. R^2 (%)	8.65	8.70	8.85	8.38	8.68
No. of Obs	292	292	292	292	292

Table 7: We consider the 90% quantile of the highest absolute SPX futures returns in the rebalancing window. The table reports regression results for the model in (27). All variables are standardized. Newey-West t-statistics are presented in parentheses, and ***, **, * indicates 1%, 5%, and 10% significance, respectively.

For the delta hedging effect, we observe that the t-statistics are similar to the previous regressions, while the estimated coefficient magnitude is drastically increased. This indicates that the hedging effect is an exceedingly pronounced predictor, in particular compared to the control variables, when the end-of-day market is moving significantly to either direction.

Furthermore, by repeating the exercise with the delta effect decomposed, we observe from Table 8 that the coefficients for both components increase in absolute magnitude. The gamma effect remains statistically robust, while the inventory effect gains in significance. This indicates that in periods of market turmoil, the hedging of new option positions becomes a more important driver of end-of-day futures returns.

In Figure 2, it is evident that the market maker's option inventory is generally more balanced towards the end of the sample, in particular after 2020. As a robustness check, we revisit the above daily regressions for a sample period ending just before Corona. The regression results are provided in Appendix A, and the conclusions are robust to the change in the sample period.

Moreover, in Appendix B, we repeat the analysis by classifying trades with the quote rule.

[3]Positive returns are recorded on 43% of the days, while the remaining days have negative returns.

$r_{t,15.45-16.15}$	(1)	(2)	(3)	(4)	(5)	(6)	(7)
$\delta_{t,15.45}(N_{t,15.45} - N_{t-1,16.15})$	-0.212** (-2.241)		-0.226** (-2.295)	-0.223** (-2.093)	-0.236** (-2.451)	-0.225** (-2.293)	-0.231** (-2.237)
$N_{t-1,16.15}(\delta_{t,15.45} - \delta_{t-1,16.15})$		-0.197*** (-3.117)	-0.212*** (-3.477)	-0.201*** (-3.498)	-0.220*** (-3.537)	-0.214*** (-3.387)	-0.210*** (-3.583)
$r_{t-1,16.15-t,15.45}$				0.062 (0.585)			0.066 (0.598)
$Vol^{SPX}_{t,9.30-15.45}$					0.091 (1.311)		0.087 (1.189)
$Vol^{ES}_{t,9.30-15.45}$					-0.071 (-0.706)		-0.072 (-0.751)
$RV_{t,9.30-15.45}$						0.022 (0.335)	0.040 (0.553)
Adj. R^2 (%)	4.16	3.57	8.35	8.40	8.56	8.08	8.38
No. of Obs	292	292	292	292	292	292	292

Table 8: We consider the 90% quantile of the highest absolute SPX futures returns in the rebalancing window. The table reports regression results for the model in (28) with the delta hedging effect decomposed. All variables are standardized. Newey-West t-statistics are presented in parenthesis, and ***, **, * indicates 1%, 5% and 10% significance, respectively.

Although, the difference between the two approaches is minimal, the results are more convincing using the new GSU trade classification algorithm, which is promising as the classification accuracy is significantly increased (Grauer et al. 2023). In all cases, the change in option market maker's net delta position is a statistically strong predictor of end-of-day SPX futures return.

4.4 Intraday hedging

We previously argued that the market maker has reasons to refrain from hedging during the trading day. However, when the shocks to the market maker's delta position are sufficiently large, it may be too risky to postpone the hedging until the end of the day. We conjecture that significant changes in the market maker's net delta position will offset an immediate hedge. The effect should be negative, such that a positive change is neutralized by selling the underlying, creating negative price pressure, and the opposite being the case for a negative change in net delta. Hence, we experiment with a threshold on the net delta change, and consider the α% largest absolute moves in net delta exposure on a 5-minute granularity. The 5-minute frequency is chosen as it gives the market maker sufficient time to react to substantial option

trades. Panel A in Table 9 reports the outcome of the regressions for different cut of levels of the threshold. The coefficient on the net delta difference is particularly interesting, as it increases (in absolute terms) when the threshold becomes stricter. This indicates that the OMM hedges more aggressively in the SPX futures market after large changes to the delta position. As a robustness check, we also include the return in the succeeding time interval as control variable, and we observe that the impact remains when controlling for momentum. While the significance level is not below the 1% threshold, the t-statistics appear stable across α-threshold.

Panel A: Upper quantiles										
$r_{t,t+5\text{min}}$	$\alpha = 10\%$		$\alpha = 5\%$		$\alpha = 2.5\%$		$\alpha = 1\%$		$\alpha = 0.1\%$	
$\Delta_t - \Delta_{t-5\text{min}}$	-0.079**	-0.084**	-0.111**	-0.127**	-0.148**	-0.164**	-0.209*	-0.228*	-0.336*	-0.360*
	(-2.289)	(-2.306)	(-2.304)	(-2.449)	(-2.190)	(-2.384)	(-1.852)	(-1.903)	(-1.757)	(-1.823)
$r_{t-5\text{min},t}$		-0.023		-0.071**		-0.073*		-0.104		-0.239
		(-0.900)		(-2.440)		(-1.696)		(-1.338)		(-1.602)
Adj. R^2 (%)	0.62	0.66	1.22	1.69	2.17	2.66	4.31	5.30	10.86	16.13
No. of Obs	21539	21539	10769	10769	5383	5383	2151	2151	216	216
Panel B: Lower quantiles										
$r_{t,t+5\text{min}}$	$\beta = 0.1\%$		$\beta = 1\%$		$\beta = 2.5\%$		$\beta = 5\%$		$\beta = 10\%$	
$\Delta_t - \Delta_{t-5\text{min}}$	-0.017	-0.010	-0.019	-0.018	0.008	0.010	-0.013	-0.012	-0.009	-0.009
	(-0.737)	(-0.375)	(-1.132)	(-0.965)	(0.654)	(0.835)	(-1.466)	(-1.428)	(-1.377)	(-1.377)
$r_{t-5\text{min},t}$		-0.156		-0.089		-0.086		-0.035		-0.012
		(-0.443)		(-0.722)		(-1.267)		(-0.896)		(-0.507)
Adj. R^2 (%)	-0.51	1.42	-0.01	0.74	-0.01	0.71	0.01	0.12	0.00	0.01
No. of Obs	189	189	2127	2127	5358	5358	10745	10745	21518	21518

Table 9: Analysis of the entire sample on 5-minute frequency, excluding the end-of-day window. All variables are standardized. Newey-West t-statistics are presented in parentheses, and ***, **, * indicates 1%, 5%, and 10% significance, respectively. The sample sorting is based on upper α-quantiles and lower β-quantiles of the net delta position changes.

Moreover, we analyze the impact of delta hedging by decomposing the net delta difference into the gamma effect and the inventory effect and run the regressions again on subsamples defined by large movements in the delta exposure. The findings are presented in Panel A in Table 10, where we observe that only the inventory effect is significant. Similarly, we run the regressions on subsamples defined by the $\beta\%$ *smallest* absolute changes in the delta exposure and report the results in Panel B of Tables 9-10. When focusing the attention on small delta position changes, we find that neither the inventory effect nor the gamma effect has an impact. Tables 6 and 10 provide evidence that delta hedging activities related to the gamma effect are postponed until market close while large changes to the option inventory are hedged immedi-

ately by the OMM. In addition, hedging of smaller changes to the option inventory is postponed until market close.

Panel A: Upper quantiles															
$r_{t,t+5\,\text{min}}$	$\alpha = 10\%$			$\alpha = 5\%$			$\alpha = 2.5\%$			$\alpha = 1\%$			$\alpha = 0.1\%$		
$\delta_t(N_t - N_{t-5min})$	-0.074**		-0.067**	-0.105**		-0.097**	-0.141**		-0.129**	-0.201*		-0.185**	-0.342*		-0.334**
	(-2.346)		(-2.326)	(-2.387)		(-2.472)	(-2.233)		(-2.362)	(-1.927)		(-2.086)	(-1.932)		(-2.208)
$N_{t-5min}(\delta_t - \delta_{t-5min})$		-0.048	-0.034		-0.068	-0.058		-0.090	-0.067		-0.126	-0.083		-0.190	-0.066
		(-1.471)	(-1.194)		(-1.411)	(-1.284)		(-1.353)	(-1.235)		(-1.284)	(-1.051)		(-1.109)	(-0.671)
$r_{t-5\,\text{min},t}$			-0.024			-0.073**			-0.075			-0.103			-0.237
			(-0.887)			(-2.369)			(-1.558)			(-1.340)			(-1.555)
Adj. R^2 (%)	0.55	0.22	0.66	1.09	0.45	1.69	1.96	0.80	2.65	3.98	1.55	5.25	11.31	3.15	16.30
No. of Obs	21539	21539	21539	10769	10769	10769	5383	5383	5383	2151	2151	2151	216	216	216
Panel B: Lower quantiles															
$r_{t,t+5\,\text{min}}$	$\beta = 0.1\%$			$\beta = 1\%$			$\beta = 2.5\%$			$\beta = 5\%$			$\beta = 10\%$		
$\delta_t(N_t - N_{t-5min})$	0.010		-9.283	-0.025		-1.063	-0.029*		0.215	-0.018		-0.149	-0.012		-0.056
	(0.208)		(-0.372)	(-1.123)		(-0.958)	(-1.652)		(0.765)	(-1.524)		(-1.498)	(-1.417)		(-1.481)
$N_{t-5min}(\delta_t - \delta_{t-5min})$		-0.010	-9.283		0.025	-1.038		0.029*	0.243		0.016	-0.132		0.010	-0.045
		(-0.208)	(-0.371)		(1.107)	(-0.932)		(1.672)	(0.865)		(1.427)	(-1.319)		(1.231)	(-1.176)
$r_{t-5\,\text{min},t}$			-0.156			-0.089			-0.086			-0.035			-0.012
			(-0.440)			(-0.724)			(-1.263)			(-0.897)			(-0.514)
Adj. R^2 (%)	-0.53	-0.53	0.88	0.02	0.01	0.75	0.07	0.07	0.78	0.02	0.02	0.14	0.01	0.01	0.02
No. of Obs	189	189	189	2127	2127	2127	5358	5358	5358	10745	10745	10745	21518	21518	21518

Table 10: Analysis of the entire sample on 5-minute frequency, excluding the end-of-day window and with the net delta change decomposed. All variables are standardized. Newey-West t-statistics are presented in parentheses, and ***, **, * indicates 1%, 5%, and 10% significance, respectively. The sample sorting is based on upper α-quantiles and lower β-quantiles of the net delta position changes.

4.4.1 Large intraday movements in SPX futures returns

In this subsection, contrary to sorting by the largest shocks to the market maker's delta position, we focus on the top α% of absolute SPX futures returns at 5-minute intervals. Thus, when the intraday market moves rapidly, we examine the importance of the delta component. As demonstrated in Table 11, the predictive effect is a non-negligible factor of the most volatile high-frequency returns. Furthermore, the significance level is constant across varying α, while the coefficient on the hedging impact increases absolutely.

Table 12 reports the outcome of repeating the analysis with the decomposed delta hedging effect. The analysis reveals similar conclusions as above: the inventory effect is the primary driver of market maker intraday hedging.

$r_{t,t+5\text{min}}$	$\alpha = 10\%$		$\alpha = 5\%$		$\alpha = 2.5\%$		$\alpha = 1\%$		$\alpha = 0.1\%$	
$\Delta_t - \Delta_{t-5\text{min}}$	-0.073*** (-2.952)	-0.076*** (-2.993)	-0.081*** (-2.753)	-0.085*** (-2.838)	-0.095*** (-2.844)	-0.100*** (-2.881)	-0.136*** (-3.754)	-0.143*** (-4.000)	-0.250*** (-3.661)	-0.250*** (-3.616)
$r_{t-5\text{min},t}$		-0.024 (-1.634)		-0.031* (-1.704)		-0.046** (-1.991)		-0.065** (-2.104)		-0.018 (-0.240)
Adj. R^2 (%)	0.52	0.57	0.65	0.74	0.88	1.07	1.81	2.18	5.84	5.44
No. of Obs	21807	21807	10907	10907	5453	5453	2182	2182	218	218

Table 11: Analysis of the entire sample on 5-minute frequency, excluding the end-of-day window. All variables are standardized. Newey-West t-statistics are presented in parentheses, and ***, **, * indicates 1%, 5%, and 10% significance, respectively. The sample sorting is based on quantiles of the intraday SPX futures return.

$r_{t,t+5\text{min}}$	$\alpha = 10\%$			$\alpha = 5\%$			$\alpha = 2.5\%$			$\alpha = 1\%$			$\alpha = 0.1\%$		
$\delta_t(N_t - N_{t-5min})$	-0.070*** (-3.479)		-0.061*** (-3.786)	-0.079*** (-3.273)		-0.067*** (-3.694)	-0.094*** (-3.444)		-0.080*** (-4.098)	-0.129*** (-3.424)		-0.103*** (-4.930)	-0.221*** (-2.608)		-0.144*** (-3.676)
$N_{t-5min}(\delta_t - \delta_{t-5min})$		-0.047** (-2.071)	-0.026 (-1.274)		-0.056** (-2.022)	-0.028 (-1.073)		-0.067** (-1.989)	-0.029 (-0.883)		-0.096** (-2.023)	-0.065 (-1.644)		-0.233*** (-3.600)	-0.169** (-2.509)
$r_{t-5\text{min},t}$			-0.024 (-1.548)			-0.031 (-1.611)			-0.045* (-1.899)			-0.069** (-2.158)			-0.024 (-0.333)
Adj. R^2 (%)	0.49	0.21	0.57	0.62	0.30	0.73	0.86	0.43	1.05	1.62	0.88	2.17	4.45	4.99	5.91
No. of Obs	21807	21807	21807	10907	10907	10907	5453	5453	5453	2182	2182	2182	218	218	218

Table 12: Similar to Table 11 with decomposed delta effect. All variables are standardized. Newey-West t-statistics are presented in parentheses, and ***, **, * indicates 1%, 5%, and 10% significance, respectively. The sample sorting is based on quantiles of the intraday SPX futures return.

5 Conclusion

We propose a model that captures the impact of Options Market Makers (OMMs) delta hedging their option inventory. A similar approach is followed in Sornette et al. (2022), where the impact materializes when OMMs update their hedges in reaction to price changes in the underlying security (the gamma effect). We extend their model by including an impact when changes to the option inventory are hedged by the OMM. When the fundamental value of the stock price has constant volatility and drift, inclusion of a linear hedging impact implies that the observable stock price features both stochastic volatility and stochastic drift terms. We show via simulation that the hedging impact is significant and that the impact of changes to the option inventory is sizable. Focusing on the trading impact implied by the gamma effect in isolation will underestimate the impact in scenarios where the OMM's option inventory changes in a direction that implies trading in the same direction as the gamma effect, while it will overestimate it when the adjustments move in the opposite direction. We provide empirical

support for the model predictions using a high-frequency data set on SPX option trades over an extended period. We find that the change in the delta position of the OMM is a significant predictor of the end-of-day return on SPX futures. A decomposition of the change in the delta position into components implied by the gamma effect and adjustments resulting from variations in the option inventory reveals that both quantities are highly significant and with impact in line with the model predictions. An analysis of the hedging impact on an intradaily 5-minute horizon reveals that the market impact is increasing in the hedging demand. Finally, the decomposition of the delta change provides evidence that delta hedging activities related to the gamma effect are postponed until market close while large changes to the option inventory are hedged immediately by the OMM. In addition, hedging of smaller changes to the option inventory is postponed until market close.

Acknowledgement

The research presented in this paper has been conducted with support from the Independent Research Fund Denmark (Grant: DFF 0133-00151B). The authors wish to thank Christine Bangsgaard, Hans Buehler, Bent Jesper Christensen, Niels Strange Grønborg, Elisa Nicolato, Rolf Poulsen, Alessandro Previtero, and Angel Serrat for useful comments. The paper has been presented at the XXV Workshop on Quantitative Finance, Bologna, 2024, the 12th Bachelier World Congress of the Bachelier Finance Society, Rio, 2024, the Symposium in honor of Jørgen Aase Nielsen, Aarhus, 2024, the 14th International Conference of the Financial Engineering and Banking Society, Montpellier, 2025, and the CoRE Workshop on Stochastic Finance and Machine Learning, Aarhus, 2025.

Disclosure statement

No potential conflict of interest was reported by the authors.

References

Almgren, R., Thum, C., Hauptmann, E., and Li, H. (2005). Direct estimation of equity market impact. *Risk*, 18(7):58–62.

Avellaneda, M. and Lipkin, M. (2003). A market-induced mechanism for stock pinning. *Quantitative Finance*, 3(6):417–425.

Baltussen, G., Da, Z., Lammers, S., and Martens, M. (2021). Hedging demand and market intraday momentum. *Journal of Financial Economics*, 142(1):377–403.

Bangsgaard, C. and Kokholm, T. (2024). The lead-lag relation between VIX futures and SPX futures. *Journal of Financial Markets*, 67:100851.

Bangsgaard, C. and Kokholm, T. (2025). The stock market impact of volatility hedging: Evidence from end-of-day trading by VIX ETPs. *Journal of Banking & Finance*, 180:107556.

Barbon, A., Beckmeyer, H., Buraschi, A., and Moerke, M. (2021). Liquidity provision to leveraged ETFs and equity options rebalancing flows: Evidence from end-of-day stock prices. *Available at SSRN 3925725*.

Barbon, A. and Buraschi, A. (2020). Gamma fragility. *Available at SSRN 3725454*.

Barndorff-Nielsen, O. E., Hansen, P. R., Lunde, A., and Shephard, N. (2009). Realized kernels in practice: Trades and quotes. *Econometrics Journal*, 12(3):C1–C32.

Bollen, N. P. and Whaley, R. E. (2004). Does net buying pressure affect the shape of implied volatility functions? *The Journal of Finance*, 59(2):711–753.

Bouchaud, J.-P., Farmer, J. D., and Lillo, F. (2009). How markets slowly digest changes in supply and demand. In *Handbook of financial markets: dynamics and evolution*, pages 57–160. Elsevier.

Bryzgalova, S., Pavlova, A., and Sikorskaya, T. (2023). Retail trading in options and the rise of the big three wholesalers. *The Journal of Finance*, 78(6):3465–3514.

Chen, W.-P., Chung, H., and Lien, D. (2016). Price discovery in the S&P 500 index derivatives markets. *International Review of Economics & Finance*, 45:438–452.

Christoffersen, P., Goyenko, R., Jacobs, K., and Karoui, M. (2018). Illiquidity premia in the equity options market. *The Review of Financial Studies*, 31(3):811–851.

Easley, D., Lopez de Prado, M., and O'Hara, M. (2016). Discerning information from trade data. *Journal of Financial Economics*, 120(2):269–285.

Gao, L., Han, Y., Li, S. Z., and Zhou, G. (2018). Market intraday momentum. *Journal of Financial Economics*, 129(2):394–414.

Garleanu, N., Pedersen, L. H., and Poteshman, A. M. (2008). Demand-based option pricing. *The Review of Financial Studies*, 22(10):4259–4299.

Golez, B. and Jackwerth, J. C. (2012). Pinning in the S&P 500 futures. *Journal of Financial Economics*, 106(3):566–585.

Goyenko, R. and Zhang, C. (2019). Option returns: Closing prices are not what you pay. *Unpublished working paper. McGill University*.

Grauer, C., Schuster, P., and Uhrig-Homburg, M. (2023). Option trade classification. *Available at SSRN 4098475*.

Grossman, S. J. and Miller, M. H. (1988). Liquidity and market structure. *The Journal of Finance*, 43(3):617–633.

Heston, S. L., Korajczyk, R. A., and Sadka, R. (2010). Intraday patterns in the cross-section of stock returns. *The Journal of Finance*, 65(4):1369–1407.

Ho, T. and Stoll, H. R. (1981). Optimal dealer pricing under transactions and return uncertainty. *Journal of Financial economics*, 9(1):47–73.

Hong, H. and Wang, J. (2000). Trading and returns under periodic market closures. *The Journal of Finance*, 55(1):297–354.

Hu, J. (2014). Does option trading convey stock price information? *Journal of Financial Economics*, 111(3):625–645.

Jacobs, K. and Mai, A. T. (2024). The role of intermediaries in derivatives markets: Evidence from VIX options. *Journal of Empirical Finance*, 77:101492.

Lee, C. M. and Ready, M. J. (1991). Inferring trade direction from intraday data. *The Journal*

of Finance, 46(2):733–746.

Lillo, F., Farmer, J. D., and Mantegna, R. N. (2003). Master curve for price-impact function. *Nature*, 421(6919):129–130.

Muravyev, D. and Ni, X. C. (2020). Why do option returns change sign from day to night? *Journal of Financial Economics*, 136(1):219–238.

Ni, S. X., Pearson, N. D., and Poteshman, A. M. (2005). Stock price clustering on option expiration dates. *Journal of Financial Economics*, 78(1):49–87.

Ni, S. X., Pearson, N. D., Poteshman, A. M., and White, J. (2021). Does option trading have a pervasive impact on underlying stock prices? *Review of Financial Studies*, 34(4):1952–1986.

Patzelt, F. and Bouchaud, J.-P. (2018). Universal scaling and nonlinearity of aggregate price impact in financial markets. *Physical Review E*, 97(1):012304.

Protter, P. (1990). *Stochastic integration and differential equations*. Springer-Verlag.

Sornette, D., Ulmann, F., and Wehrli, A. (2022). On the directional destabilizing feedback effects of option hedging. *Swiss Finance Institute Research Paper*, (22-34).

Stoll, H. R. and Whaley, R. E. (1987). Program trading and expiration-day effects. *Financial Analysts Journal*, 43(2):16–28.

Xu, C. (2014). Expiration-day effects of stock and index futures and options in Sweden: The return of the witches. *Journal of Futures Markets*, 34(9):868–882.

A Pre-Covid data

In our data set, we define pre-Covid as the period from January 3, 2012 to December 31, 2019.

	(1)	(2)	(3)	(4)	(5)
$\Delta_{t,15.45}$ - $\Delta_{t-1,16.15}$	-0.096***	-0.075***	-0.088***	-0.090***	-0.076***
	(-3.685)	(-3.415)	(-3.452)	(-3.659)	(-3.298)
$r_{t-1,16.15-t,15.45}$		0.092*			0.063
		(1.954)			(1.518)
$Vol^{SPX}_{t,9.30-15.45}$			-0.038		-0.025
			(-0.924)		(-0.764)
$Vol^{ES}_{t,9.30-15.45}$			-0.111**		-0.043
			(-2.427)		(-0.792)
$RV_{t,9.30-15.45}$				-0.134*	-0.077
				(-1.731)	(-0.797)
Adj. R^2 (%)	0.87	1.62	2.42	2.60	2.96
No. of Obs	2006	2006	2006	2006	2006

Table A.1: SPX futures return in the hedging window with pre-Covid data. The table replicates Table 4 with the GSU trade classification algorithm. All variables are standardized. Newey-West t-statistics are presented in parentheses, and ***, **, * indicates 1%, 5%, and 10% significance, respectively.

	(1)	(2)	(3)	(4)	(5)	(6)	(7)
$\delta_{t,15.45}(N_{t,15.45} - N_{t-1,16.15})$	-0.069***		-0.072***	-0.051**	-0.066**	-0.057**	-0.049*
	(-2.709)		(-2.818)	(-2.058)	(-2.427)	(-2.229)	(-1.814)
$N_{t-1,16.15}(\delta_{t,15.45} - \delta_{t-1,16.15})$		-0.068***	-0.071***	-0.060***	-0.066***	-0.074***	-0.062***
		(-2.912)	(-2.985)	(-2.859)	(-2.934)	(-3.006)	(-2.817)
$r_{t-1,16.15-t,15.45}$				0.090*			0.062
				(1.888)			(1.473)
$Vol^{SPX}_{t,9.30-15.45}$					-0.044		-0.028
					(-1.035)		(-0.828)
$Vol^{ES}_{t,9.30-15.45}$					-0.107**		-0.042
					(-2.337)		(-0.787)
$RV_{t,9.30-15.45}$						-0.133*	-0.076
						(-1.694)	(-0.775)
Adj. R^2 (%)	0.42	0.41	0.88	1.58	2.42	2.57	2.92
No. of Obs	2006	2006	2006	2006	2006	2006	2006

Table A.2: SPX futures return in the hedging window with pre-Covid data. The table replicates Table 6 with the decomposed change in net delta and the GSU trade classification algorithm. All variables are standardized. Newey-West t-statistics are presented in parentheses, and ***, **, * indicates 1%, 5%, and 10% significance, respectively.

	(1)	(2)	(3)	(4)	(5)
$\Delta_{t,15.45}$ - $\Delta_{t-1,16.15}$	-0.287***	-0.222***	-0.267***	-0.286***	-0.244***
	(-3.943)	(-3.403)	(-4.219)	(-4.373)	(-3.755)
$r_{t-1,16.15-t,15.45}$		0.161*			0.099
		(1.770)			(1.243)
$Vol^{SPX}_{t,9.30-15.45}$			0.011		0.069
			(0.134)		(0.784)
$Vol^{ES}_{t,9.30-15.45}$			-0.192**		-0.090
			(-1.990)		(-1.035)
$RV_{t,9.30-15.45}$				-0.191	-0.146
				(-1.429)	(-0.914)
Adj. R^2 (%)	7.77	9.49	10.33	11.00	11.19
No. of Obs	201	201	201	201	201

Table A.3: The table replicates Table 7 using pre-Covid data with the 90% quantile of the highest absolute end-of-day SPX futures returns in the hedging window and the GSU trade classification algorithm. All variables are standardized. Newey-West t-statistics are presented in parentheses, and ***, **, * indicates 1%, 5%, and 10% significance, respectively.

	(1)	(2)	(3)	(4)	(5)	(6)	(7)
$\delta_{t,15.45}(N_{t,15.45} - N_{t-1,16.15})$	-0.160**		-0.175***	-0.113	-0.150**	-0.172**	-0.119
	(-2.431)		(-2.672)	(-1.602)	(-2.250)	(-2.567)	(-1.629)
$N_{t-1,16.15}(\delta_{t,15.45} - \delta_{t-1,16.15})$		-0.229***	-0.240***	-0.199***	-0.233***	-0.240***	-0.222***
		(-3.142)	(-3.424)	(-3.332)	(-3.813)	(-3.988)	(-3.822)
$r_{t-1,16.15-t,15.45}$				0.166*			0.106
				(1.761)			(1.269)
$Vol^{SPX}_{t,9.30-15.45}$					0.016		0.080
					(0.187)		(0.875)
$Vol^{ES}_{t,9.30-15.45}$					-0.197**		-0.095
					(-1.995)		(-1.085)
$RV_{t,9.30-15.45}$						-0.191	-0.147
						(-1.426)	(-0.917)
Adj. R^2 (%)	2.06	4.75	7.34	9.14	9.96	10.59	10.92
No. of Obs	201	201	201	201	201	201	201

Table A.4: The table replicates Table 8 using pre-Covid data with the 90% quantile of the highest absolute end-of-day SPX futures returns in the hedging window, the decomposed change in net delta and the GSU trade classification algorithm. All variables are standardized. Newey-West t-statistics are presented in parentheses, and ***, **, * indicates 1%, 5%, and 10% significance, respectively.

B Trade classification algorithm

	(1)	(2)	(3)	(4)	(5)
$\Delta_{t,15.45}$ - $\Delta_{t-1,16.15}$	-0.080***	-0.073***	-0.078***	-0.076***	-0.074***
	(-3.195)	(-2.823)	(-2.948)	(-2.652)	(-2.723)
$r_{t-1,16.15-t,15.45}$		0.057			0.043
		(1.220)			(0.903)
$Vol^{SPX}_{t,9.30-15.45}$			0.022		0.027
			(0.993)		(1.214)
$Vol^{ES}_{t,9.30-15.45}$			-0.073*		-0.048
			(-1.910)		(-1.295)
$RV_{t,9.30-15.45}$				-0.056	-0.025
				(-1.380)	(-0.598)
Adj. R^2 (%)	0.61	0.90	1.02	0.88	1.17
No. of Obs	2917	2917	2917	2917	2917

Table B.1: The table replicates Table 4 using the quote rule for trade classification rather than the GSU algorithm. All variables are standardized. Newey-West t-statistics are presented in parentheses, and ***, **, * indicates 1%, 5%, and 10% significance, respectively.

	(1)	(2)	(3)	(4)	(5)	(6)	(7)
$\delta_{t,15.45}(N_{t,15.45} - N_{t-1,16.15})$	-0.072*		-0.076*	-0.071*	-0.076*	-0.068	-0.073
	(-1.855)		(-1.956)	(-1.794)	(-1.753)	(-1.600)	(-1.632)
$N_{t-1,16.15}(\delta_{t,15.45} - \delta_{t-1,16.15})$		-0.045***	-0.051***	-0.046***	-0.050***	-0.051***	-0.047***
		(-2.984)	(-3.320)	(-3.120)	(-3.300)	(-3.095)	(-3.151)
$r_{t-1,16.15-t,15.45}$				0.057			0.043
				(1.192)			(0.897)
$Vol^{SPX}_{t,9.30-15.45}$					0.030		0.034
					(1.110)		(1.260)
$Vol^{ES}_{t,9.30-15.45}$					-0.072*		-0.050
					(-1.886)		(-1.316)
$RV_{t,9.30-15.45}$						-0.052	-0.022
						(-1.242)	(-0.526)
Adj. R^2 (%)	0.48	0.17	0.71	0.99	1.12	0.94	1.26
No. of Obs	2917	2917	2917	2917	2917	2917	2917

Table B.2: The table replicates Table 6 using the quote rule for trade classification rather than the GSU algorithm. All variables are standardized. Newey-West t-statistics are presented in parentheses, and ***, **, * indicates 1%, 5%, and 10% significance, respectively.

	(1)	(2)	(3)	(4)	(5)
$\Delta_{t,15.45}$ - $\Delta_{t-1,16.15}$	-0.256***	-0.248***	-0.274***	-0.257***	-0.265***
	(-3.177)	(-2.718)	(-3.229)	(-2.966)	(-2.847)
$r_{t-1,16.15-t,15.45}$		0.079			0.085
		(0.746)			(0.766)
$Vol^{SPX}_{t,9.30-15.45}$			0.098		0.097
			(1.386)		(1.264)
$Vol^{ES}_{t,9.30-15.45}$			-0.074		-0.070
			(-0.745)		(-0.733)
$RV_{t,9.30-15.45}$				0.018	0.037
				(0.316)	(0.522)
Adj. R^2 (%)	6.25	6.54	6.55	5.96	6.61
No. of Obs	292	292	292	292	292

Table B.3: The table replicates Table 7 using the quote rule for trade classification rather than the GSU algorithm. All variables are standardized. Newey-West t-statistics are presented in parentheses, and ***, **, * indicates 1%, 5%, and 10% significance, respectively.

	(1)	(2)	(3)	(4)	(5)	(6)	(7)
$\delta_{t,15.45}(N_{t,15.45} - N_{t-1,16.15})$	-0.186*		-0.201**	-0.201*	-0.218**	-0.200**	-0.216**
	(-1.877)		(-1.976)	(-1.834)	(-2.162)	(-1.982)	(-1.997)
$N_{t-1,16.15}(\delta_{t,15.45} - \delta_{t-1,16.15})$		-0.161**	-0.178***	-0.164***	-0.186***	-0.179***	-0.174***
		(-2.472)	(-2.868)	(-2.803)	(-2.901)	(-2.783)	(-2.877)
$r_{t-1,16.15-t,15.45}$				0.080			0.086
				(0.759)			(0.778)
$Vol^{SPX}_{t,9.30-15.45}$					0.099		0.097
					(1.380)		(1.259)
$Vol^{ES}_{t,9.30-15.45}$					-0.075		-0.071
					(-0.744)		(-0.734)
$RV_{t,9.30-15.45}$						0.018	0.037
						(0.275)	(0.500)
Adj. R^2 (%)	3.12	2.24	5.94	6.25	6.25	5.65	6.32
No. of Obs	292	292	292	292	292	292	292

Table B.4: The table replicates Table 8 using the quote rule for trade classification rather than the GSU algorithm. All variables are standardized. Newey-West t-statistics are presented in parentheses, and ***, **, * indicates 1%, 5%, and 10% significance, respectively.